

Learning Causal States Under Partial Observability and Perturbation

Na Li, *Graduate Student Member, IEEE*, Hangguan Shan, *Senior Member, IEEE*, Wei Ni, *Fellow, IEEE*,
Wenjie Zhang, *Senior Member, IEEE*, Xinyu Li, *Member, IEEE*, and Yamin Wang

Abstract—A critical challenge for reinforcement learning (RL) is making decisions based on incomplete and noisy observations, especially in perturbed and partially observable Markov decision processes (P²OMDPs). Existing methods fail to mitigate perturbations while addressing partial observability. We propose *Causal State Representation under Asynchronous Diffusion Model (CaDiff)*, a framework that enhances any RL algorithm by uncovering the underlying causal structure of P²OMDPs. This is achieved by incorporating a novel asynchronous diffusion model (ADM) and a new bisimulation metric. ADM enables forward and reverse processes with different numbers of steps, thus interpreting the perturbation of P²OMDP as part of the noise suppressed through diffusion. The bisimulation metric quantifies the similarity between partially observable environments and their causal counterparts. Moreover, we establish the theoretical guarantee of CaDiff by deriving an upper bound for the value function approximation errors between perturbed observations and denoised causal states, reflecting a principled trade-off between approximation errors of reward and transition-model. Experiments on Roboschool tasks show that CaDiff enhances returns by at least 14.18% compared to baselines. CaDiff is the first framework that approximates causal states using diffusion models with both theoretical rigor and practicality.

Index Terms—Reinforcement learning, perturbed partially observable Markov decision process (P²OMDP), causal inference, state representation, diffusion model.

I. INTRODUCTION

PARTIALLY observable Markov decision processes (POMDPs) are relevant to a wide range of real-world applications, such as robotics, autonomous driving, and finance [1]. Perturbed POMDPs (P²OMDPs) have been generally challenging for deep reinforcement learning (DRL), where deep RL (DRL) agents must make optimal decisions under both incomplete state observations and additional perturbations caused by sensor noise, environmental disruptions, or discrepancies between training datasets and actual conditions. This noise complicates state inference by masking essential features or introducing false signals.

Causal state extraction has offered an effective means to capture the essential relationships between past observations and future returns, filter out irrelevant data, and contribute to improved efficiency. Existing studies have been primarily based on Markov decision processes (MDPs) [2], with little effort on POMDPs. Let alone P²OMDPs, where noise can comprise causal state extraction from the partially observable states. While it is possible to denoise the perturbed partially observed states, balancing between denoising and preserving the original causal structure is vital.

Diffusion models (DMs), as the state-of-the-art generative models, have offered effective denoising capability. DMs [3] are adept at removing noise while preserving essential data features, through an iterative process that transforms

noisy samples into high-quality, real samples. In contrast, traditional generative model-based approaches, which are integrated into POMDPs through algorithms, including deep variational RL [4] and structured sequential variational auto-encoders [5], often generate samples by learning latent data representations, as opposed to tackling noise. DMs have gained significant attention in decision-making tasks, utilized as trajectory generators or tools for state representation [6]–[8], but have not accounted for causality.

Bisimulation offers a rigorous mathematical framework for evaluating state equivalence based on outcomes. Research on causal state representation (CSR) has been developed to extract abstract features from perturbed observations. Leveraging these abstract representations (instead of raw data) has enhanced decision-making efficiency in both MDPs [9] and POMDPs [10]. Related approaches include bisimulation-based methods [11], Kalman filters [12], ordinary differential equation-based recurrent models [13], world models [14], and studies establishing a connection between predictive state representations and bisimulation via causal states [10]. However, no existing methods have captured the impact of perturbations.

A. Contribution

This paper enhances the decision-making of DRL for P²OMDPs by extracting and denoising causal states. A novel approach, *Causal State Representation under Asynchronous Diffusion Model (CaDiff)*, is proposed to mitigate perturbations and uncover causality within denoised and partially observable states of P²OMDPs. CaDiff offers a generic framework for any RL algorithm, with the following contributions:

Algorithm Design: Tailored for P²OMDPs, CaDiff enhances any DRL operating with noisy and incomplete observations and noisy rewards, by designing a *novel asynchronous diffusion model (ADM)* and a *new bisimulation metric*.

- *ADM* enables forward and reverse processes with different numbers of steps in an asynchronous setting. Less noise is injected via fewer steps in the forward process than the noise suppressed in the reverse process, suppressing the noisy perturbation of P²OMDPs. The difference in the number of steps is regulated by noise intensity, effectively denoising each dimension of the observation features and preserving inherent causality.
- *The new bisimulation metric* quantifies the similarity between a partially observable environment and its causal state. This metric, grounded in the consistency of input states and rewards, measures the alignment between underlying distributions of transition dynamics and rewards. By incorporating causal consistency constraints, the denoised causal state captures the underlying causal structure for better decision-making.

CaDiff combines causality assessment with denoising. Guided by causality measured by the new bisimulation metric, ADM effectively denoises the perturbed partial observations of POMDPs. ADM is adept at handling disturbances across various scales and serves as a standalone denoising module.

Theoretical Guarantee: We establish a statistical theoretical guarantee for CaDiff with the upper bound of the value function approximation (VFA) error derived between perturbed observations and corresponding denoised causal states in P²OMDPs. Based on the analysis incorporating the new bisimulation metric under arbitrary distribution approximation errors, the distribution estimation error of ADM is quantified using the Wasserstein distance and analyzed through initialization, score estimation, and discretization errors. We also establish a sample complexity bound of CaDiff w.r.t. the smoothness of the data distribution and the dimensions of the observation and action spaces. Compared to standard RL algorithms, the additional computational overhead by CaDiff is marginal and polynomial in the logarithm of the observation and action space dimensions.

Extensive Simulation: CaDiff is tested in six P²OMDP environments with the soft actor-critic (SAC) RL algorithm. CaDiff outperforms all baselines by at least 14.18% in return. Despite more parameters, CaDiff delivers superior early-stage training performance in five of the six environments, while ultimately achieving the highest final return across all six. The ablation studies show that state denoising is much more effective than reward denoising due to typically higher observation dimensions. CaDiff incurs a mild cost of less than 7 GFLOPs.

B. Related Work

1) *Causal State Representation:* Several studies have focused on deriving CSR for decision-making generalization under POMDPs. For instance, the authors of [10] approximated causal states in POMDPs by invariant prediction. This concept has also been explored in [15], [16]. Some studies [17], [18] leveraged DMs for causal representation by counterfactual inference or invention. Utilizing domain-invariant causal features, the authors of [19] proposed invariant causal imitation learning to address distribution shifts. Some other works, e.g., [20], proposed ensemble representations that leverage multi-modal sensor inputs to boost generalizability for self-driving agents under uncertainty quantification. The PlanT framework [21] serves as a learnable planner module grounded in object-centric representations. Moreover, the realm of RL has witnessed advancements in state representation through self-supervised learning, including hierarchical skill decomposition [22], time-contrastive learning [23], variational auto-encoder [24], confounding and causal inference [25], and deep bisimulation metric learning [11]. However, there is a lack of consideration of perturbation-based CSR.

2) *RL with DM:* DM is a generative model, initially for image generation [3]. It has been adopted in decision-making for state-based tasks, especially for perturbed states. In RL, DMs can be utilized, not only for direct decision-making [6]–[8], but also for effective denoising and distribution estimation. DMBP [8] utilizes a DM as a denoiser rather than a generator.

DIPO [26] utilizes a DM to address the denoising problem in model-free RL. The authors of [27] presented a sharp statistical theory of distribution estimation for the conditional DM. However, these studies do not differentiate the noise used for training, hence limiting the effectiveness of denoising.

To the best of our knowledge, no existing frameworks have extracted causal states of P²OMDPs, which is nontrivial and necessitates the integration of CSR with effective denoising.

II. PRELIMINARIES AND PROBLEM FORMULATION

A. Wasserstein Distance and Hölder Ball

The distance between two distributions can be measured using Wasserstein distance to measure convergence of CaDiff.

Definition 1 (Wasserstein metric [28]). *Let $d : X \times X \rightarrow [0, \infty)$ denote a distance function, and Ω denote the collection of all joint distributions on $X \times X$ whose marginals are μ and λ . The Wasserstein metric is defined as*

$$W_p(d)(\mu, \lambda) = \left(\inf_{\omega \in \Omega} \mathbb{E}_{(x_1, x_2) \sim \omega} [d(x_1, x_2)^p] \right)^{1/p}. \quad (1)$$

Definition 2 (Dual formulation of Wasserstein metric [28]). *A dual formulation of the Wasserstein metric is given by*

$$W_p(d)(\mu, \lambda) = \left(\sup_{\zeta \oplus \psi \leq d^p} \mathbb{E}_{x_1 \sim \mu} [\zeta(x_1)] + \mathbb{E}_{x_2 \sim \lambda} [\psi(x_2)] \right)^{1/p},$$

where $\zeta \oplus \psi \leq d^p$ is equivalent to $\zeta(x) + \psi(y) \leq d(x, y)^p, \forall (x, y) \in X \times X$.

In the case of $p = 1$, the dual formulation simplifies to

$$W_1(d)(\mu, \lambda) = \sup_{f \in \text{Lip}_{1,d}(X)} \mathbb{E}_{x_1 \sim \mu} [f(x_1)] - \mathbb{E}_{x_2 \sim \lambda} [f(x_2)], \quad (2)$$

where $\text{Lip}_{1,d}(X)$ denotes the set of all 1-Lipschitz functions $f : X \rightarrow \mathbb{R}$ satisfying $|f(x_1) - f(x_2)| \leq d(x_1, x_2)$.

There is a closed-form expression of Gaussian measures for the 2-Wasserstein metric $W_2(\cdot \parallel \cdot)$ (abbreviated as W_2) [29]:

$$W_2(\mathcal{N}(\mu_i, \Sigma_i), \mathcal{N}(\mu_j, \Sigma_j)) = (\|\mu_i - \mu_j\|_2^2 + \|\Sigma_i - \Sigma_j\|_{\mathcal{F}}^2)^{1/2}. \quad (3)$$

Here, $\|\cdot\|_{\mathcal{F}}$ represents the Frobenius norm. If $\Sigma_i, \Sigma_j \rightarrow 0$ (i.e., both distributions collapse to point masses), the 2-Wasserstein metric recedes to the Euclidean distance between the points.

Lemma 1 (p -Wasserstein Inequality [28]). *For any distributions μ and λ , $W_q(\mu, \lambda) \geq W_p(\mu, \lambda), \forall q \geq p$.*

Lemma 2 (Bounds on Wasserstein distance [30]). *For any distributions μ and λ on X ,*

$$W_1(\mu, \lambda) \leq W_p(\mu, \lambda) \leq \text{diam}(X; d)^{\frac{p-1}{p}} W_1(\mu, \lambda)^{\frac{1}{p}}, \forall p \geq 1, \quad (4)$$

where $\text{diam}(X; d)$ is the diameter of the metric space $(X; d)$.

To estimate the distribution of dynamic transitions for P²OMDPs, we define Hölder norm and Hölder ball, as follows:

Definition 3 (Hölder norm and Hölder ball). *Let $b = m + \gamma > 0$ represent the smoothness degree, with $m = \lfloor b \rfloor$ an integer and $\gamma \in [0, 1)$. For function $f : \mathbb{R}^{w_x} \rightarrow \mathbb{R}$ and multi-index s , we define the Hölder norm as*

$$|f|_{\mathcal{H}^b(\mathbb{R}^{w_x})} := \max_{s: \|s\|_1 \leq m} \sup_{\mathbf{x}} |\partial^s f(\mathbf{x})| + \max_{s: \|s\|_1 = m+\gamma} \sup_{\mathbf{x} \neq \mathbf{z}} \frac{|\partial^s f(\mathbf{x}) - \partial^s f(\mathbf{z})|}{\|\mathbf{x} - \mathbf{z}\|_1^\gamma}.$$

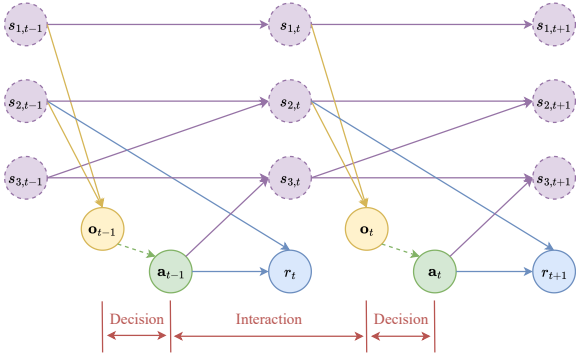


Fig. 1. System model: Solid-line and dashed-line circles denote observed and unobserved variables, respectively; solid and dashed lines represent causality and decision relationships, respectively.

A function f is said to be b -Hölder if and only if $|f|_{\mathcal{H}^b(\mathbb{R}^{w_x})} < \infty$. A Hölder ball of radius $B > 0$ is defined as

$$\mathcal{H}^b(\mathbb{R}^{w_x}, B) = \{f : \mathbb{R}^{w_x} \rightarrow \mathbb{R} \mid \|f\|_{\mathcal{H}^b(\mathbb{R}^{w_x})} < B\}.$$

B. RL for Perturbed POMDP

Environments are modeled as $\mathcal{M} = (\mathcal{S}, \mathcal{A}, \mathcal{O}, \gamma, F, G, H)$ in POMDPs, where \mathcal{S} , \mathcal{A} , and \mathcal{O} are the state, action, and observation spaces, respectively; γ is the discount factor; F , G , and H are the observation, reward, and transition functions, respectively. Consider a sequence of samples $\{\langle \mathbf{o}_t, \mathbf{a}_t, r_t \rangle\}_{t=1}^T$, where $\mathbf{o}_t \in \mathcal{O}$ is the observation at time t ; $\mathbf{a}_t \in \mathcal{A} \subseteq \mathbb{R}^{w_a}$ is the w_a -dimensional action chosen at time t ; and $r_t \in [0, 1]$ denotes the reward. Let $\mathbf{s}_t = \{s_{1,t}, \dots, s_{w_s,t}\} \in \mathcal{S}$ denote the w_s -dimensional true state. We describe the P²OMDP as the following functions and transitions:

$$\mathbf{o}_t = F(\mathbf{s}_t, \mathbf{e}_t) \iff P(\mathbf{o}_t | \mathbf{s}_t), \quad (5a)$$

$$r_t = G(\mathbf{s}_{t-1}, \mathbf{a}_{t-1}, \varepsilon_t) \iff P(r_t | \mathbf{s}_{t-1}, \mathbf{a}_{t-1}), \quad (5b)$$

$$\mathbf{s}_t = H(\mathbf{s}_{t-1}, \mathbf{a}_{t-1}, \eta_t) \iff P(\mathbf{s}_t | \mathbf{s}_{t-1}, \mathbf{a}_{t-1}), \quad (5c)$$

where \mathbf{e}_t , ε_t , and η_t are the associated independent and identically distributed (i.i.d.) random noises for each t , respectively.

Given \mathbf{a}_{t-1} and \mathbf{s}_{t-1} , state \mathbf{s}_t is independent of the states and actions occurred before time $t-1$. Action \mathbf{a}_{t-1} affects \mathbf{s}_t , but does not directly affect \mathbf{o}_t , which is affected by \mathbf{s}_t . The reward r_t is influenced by \mathbf{a}_{t-1} and \mathbf{s}_{t-1} . Let ε_t in the reward function capture noise, e.g., measurement errors.

C. Causal State Representation and Bisimulation

The structural relationships among the different dimensions of \mathbf{s}_t indicate that action \mathbf{a}_{t-1} may not affect all dimensions of \mathbf{s}_t , and the reward r_t may not be affected by all dimensions of \mathbf{s}_{t-1} . Fig. 1 shows an example with $w_s = 3$, i.e., $\mathbf{s}_t = [s_{1,t}, s_{2,t}, s_{3,t}]^T$. State $s_{3,t-1}$ affects $s_{2,t}$, but there is no connection between \mathbf{a}_{t-1} and $s_{3,t-1}$. Only $s_{2,t-1}$ has an edge towards r_t . By extracting causal state $\hat{\mathbf{s}}_t = [\hat{s}_{1,t}, \hat{s}_{2,t}]$ within the causal state space \mathcal{S}_c from \mathbf{o}_t , we suppress redundant information and retain the causal structure.

As a type of CSR, states and observations are bisimilar if they yield the same expected reward and have equivalent

Algorithm 1 CaDiff

- 1: Initialize: Discount factor γ , forward step K , noise intensity δ , observation-denoising and reward-denoising models θ and ϕ , bisimulation model ζ , and replay memory \mathcal{D} ;
- 2: **for** Epoch $t = 1, \dots, T$ **do**
- 3: Compute the (approximate) denoised causal state $\hat{\mathbf{s}}_t$ from \mathbf{o}_t using θ and ζ ;
- 4: Select action $\mathbf{a}_t \sim \pi(\hat{\mathbf{s}}_t)$, and obtain r_{t+1} and \mathbf{o}_{t+1} ;
- 5: Store transition $(\mathbf{o}_t, \mathbf{a}_t, r_{t+1}, \mathbf{o}_{t+1})$ in \mathcal{D} ;
- 6: Sample a batch of transitions \mathcal{B} randomly from \mathcal{D} ;
- 7: Obtain $\hat{\mathbf{s}}_t$ and $\hat{\mathbf{s}}_{t+1}$ from \mathbf{o}_t and \mathbf{o}_{t+1} in \mathcal{B} , respectively;
- 8: Take gradient descent on $\hat{\mathcal{L}}_{\text{State}}(\theta) + \hat{\mathcal{L}}_{\text{BS}}(\zeta)$;
- 9: Take gradient descent on $\hat{\mathcal{L}}_{\text{Rew}}(\phi) + \hat{\mathcal{L}}_{\text{BR}}(\zeta)$;
- 10: **end for**

distributions over subsequent bisimilar states and observations [31]. To this end, they exhibit a bisimulation relationship. With the environment's dynamics $P(\mathbf{s}_{t+1}, r_{t+1} | \mathbf{s}_t, \mathbf{a}_t)$, the similarity between two environments can be expressed as that between their state transition and reward functions. Following [32], equivalence in P²OMDPs is defined as follows.

Definition 4 (CSR under bisimulation). Consider a P²OMDP $\mathcal{M} = (\mathcal{S}, \mathcal{A}, \mathcal{O}, \gamma, F, G, H)$ with causal state space \mathcal{S}_c and learned encoder $\hat{F} : \mathcal{O} \rightarrow \mathcal{S}_c$. $\hat{\mathbf{s}}_t = \hat{F}(\mathbf{o}_t)$ is a causal state if, for any action \mathbf{a}_t , $P(r_{t+1} | \hat{\mathbf{s}}_t, \mathbf{a}_t) = P(r_{t+1} | \mathbf{o}_t, \mathbf{a}_t)$ and $P(\mathbf{s}_{t+1} | \hat{\mathbf{s}}_t, \mathbf{a}_t) = P(\mathbf{s}_{t+1} | \mathbf{o}_t, \mathbf{a}_t)$.

III. ALGORITHM DESIGN OF CADIFF

As summarized in Algorithm 1, the CaDiff framework consists of three modules. It employs ADM to denoise states and rewards separately. Then, it approximates causal states based on the denoised states and rewards with bisimulation. The approximated causal states and denoised rewards serve as samples for RL algorithms for decision-making.

A. Asynchronous Diffusion Model

The objective of ADM is to derive $P(\hat{\mathbf{s}}_{t+1} | \hat{\mathbf{s}}_t, \mathbf{a}_t)$ and $P(\hat{r}_{t+1} | \hat{\mathbf{s}}_t, \mathbf{a}_t)$ from $(\mathbf{o}_t, \mathbf{a}_t, r_{t+1}, \mathbf{o}_{t+1})$, where $\hat{\mathbf{s}}_{t+1}$ is the causal state estimated under denoised observations, and \hat{r}_{t+1} is the denoised reward at time $t+1$. Existing DM-based RL algorithms typically use \mathbf{o}_{t+1} and r_{t+1} as input data [8]; the distribution fitted by DM is affected by the input data's noise.

For conciseness, t and $k \in \mathbb{N}$ indicate the RL iteration and DM's step with total forward step K , respectively. ADM denoises the observations and rewards of P²OMDPs, and estimates environmental dynamics by assuming that \mathbf{o}_{t+1} and r_{t+1} are superimposed by δ -step Gaussian noise. To obtain the denoised causal state $\hat{\mathbf{s}}_{t+1}$, we input r_{t+1} and $\tilde{\mathbf{s}}_{t+1}$ to ADM, along with $\hat{\mathbf{s}}_t$ and \mathbf{o}_t , where $\tilde{\mathbf{s}}_{t+1}$ is the noised causal state. When ADM accurately predicts the future causal state, $\tilde{\mathbf{s}}_t$ serves as a sufficient statistic for the latent variables. \mathbf{x}_{t+1}^δ denotes the inputs under δ -step Gaussian noises. For simplification, we omit t . The input \mathbf{x}^δ corresponds to the results after a δ -step forward process in the DM, as follows.

Definition 5. For a P^2 OMDP, the sampled distribution P_{in} is the result of the noiseless distribution $P(\mathbf{x}_{\text{tr}}|\hat{\mathbf{s}}_t, \mathbf{a}_t)$ after δ steps of the forward process, i.e.,

$$P_{\text{in}}(\mathbf{x}^\delta|\hat{\mathbf{s}}_t, \mathbf{a}_t) = \int_{\mathbb{R}^{w_x}} P(\mathbf{x}_{\text{tr}}|\hat{\mathbf{s}}_t, \mathbf{a}_t) \sigma_\delta^{w_x} (2\pi)^{w_x/2} \times \exp\left(-\|\sqrt{\alpha_\delta}\mathbf{x}_{\text{tr}} - \mathbf{x}^\delta\|^2 / (2\sigma_\delta^2)\right) d\mathbf{x}_{\text{tr}}, \quad (6)$$

where \mathbf{x}_{tr} is the noiseless input, w_x is the dimension of input data \mathbf{x}^δ , $\alpha_\delta = 1 - \sigma_\delta^2$, and $\sigma_1^2, \dots, \sigma_K^2 > 0$ forming a predefined variance schedule.

Given the input conditional distribution $P(\mathbf{x}^\delta|\hat{\mathbf{s}}_t, \mathbf{a}_t)$, we seek for its denoised version $P(\mathbf{x}^0|\hat{\mathbf{s}}_t, \mathbf{a}_t)$. ADM adds Gaussian noise progressively through a forward diffusion process, i.e., a forward Ornstein–Uhlenbeck (OU) process as:

$$d\mathbf{x}^k = -\frac{1}{2}\mathbf{x}^k dk + d\mathbf{w}^k \quad \forall k \geq \delta \quad \text{with } \mathbf{x}^\delta \sim P(\mathbf{x}^\delta|\hat{\mathbf{s}}_t, \mathbf{a}_t); \quad (7a)$$

$$d\mathbf{x}^k = -\frac{1}{2}\mathbf{x}^k dk + d\mathbf{w}^k \quad \forall k \geq 0 \quad \text{with } \mathbf{x}^0 := \hat{\mathbf{x}}^0 = (\mathbf{x}^\delta - \sqrt{1 - \bar{\alpha}_\delta}\epsilon) / \sqrt{\bar{\alpha}_\delta}, \quad (7b)$$

where \mathbf{w}^k denotes a Wiener process, $\bar{\alpha}_\delta = \prod_{j=0}^\delta \alpha_j$ with $\alpha_j = 1 - \sigma_j^2$, and the noise ϵ is drawn from the normal distribution.

Without a step limit, \mathbf{x}^∞ converges to a Gaussian distribution. At each step k , $P(\mathbf{x}^k|\hat{\mathbf{s}}_t, \mathbf{a}_t)$ is the conditional distribution of the intermediate variable \mathbf{x}^k generated by the forward process, given the denoised causal states and actions. (7a) is a forward process that starts at step δ from the δ -step perturbed input \mathbf{x}^δ and runs $(k - \delta)$ additional steps to reach \mathbf{x}^k with $k \geq \delta$. (7b) refreshes the process with the denoised input $\hat{\mathbf{x}}^0$ at step 0 and applies the same schedule for k steps to obtain \mathbf{x}^k .

The forward process of ADM terminates at a large enough step K . The reverse process generates samples by reversing results per step in (7) as $d\bar{\mathbf{x}}^k = [\frac{1}{2}\bar{\mathbf{x}}^k + \nabla \log P(\bar{\mathbf{x}}^k|\hat{\mathbf{s}}_t, \mathbf{a}_t)] dk + d\bar{\mathbf{w}}^k$, where $\bar{\mathbf{x}}^0 \sim P(\mathbf{x}^K|\hat{\mathbf{s}}_t, \mathbf{a}_t)$; $\bar{\mathbf{w}}^k$ and $\bar{\mathbf{x}}^k$ are the time-reversed Wiener and reverse processes, respectively; $\nabla \log P(\bar{\mathbf{x}}^k|\hat{\mathbf{s}}_t, \mathbf{a}_t)$ is the unknown conditional score function and estimated utilizing conditional score networks.

In line with classifier-free guidance, a popular approach for conditional DMs [3], we define a mask variable $\tau \in \{\emptyset, \text{id}\}$ with equal probability, which determines whether the guidance is used or ignored. In this paper, we define the guidance as $\mathbf{y} = (\hat{\mathbf{s}}_t, \mathbf{a}_t)$. ADM performs conditional denoising when $\tau = \text{id}$; the guidance is omitted for the unconditional case when $\tau = \emptyset$. We further define two score-matching errors for reconstructing denoised data from P^2 OMDP, i.e., the conditional score error $\mathcal{R}(\varphi) = \frac{1}{2} \int_{k_0}^K \frac{1}{K-k_0} \mathbb{E}_{\mathbf{x}^k, \mathbf{y}} \|\varphi(\mathbf{x}^k, \mathbf{y}, k) - \nabla \log P(\mathbf{x}^k|\mathbf{y})\|_2^2 dk + \frac{1}{2} \int_\delta^K \frac{1}{K-\delta} \mathbb{E}_{\mathbf{x}^k, \mathbf{y}} \|\varphi(\mathbf{x}^k, \mathbf{y}, k) - \nabla \log P(\mathbf{x}^k|\mathbf{y})\|_2^2 dk$ for $\tau = \text{id}$ (under $\tau\mathbf{y} = \mathbf{y}$) and the unconditional score error $\mathcal{R}_0(\varphi)$ for $\tau = \emptyset$ by replacing the guidance \mathbf{y} with \emptyset in $\mathcal{R}(\varphi)$ (under $\tau\mathbf{y} = \emptyset$). Here, φ denotes the conditional score network. Unifying the two cases, we design the overall loss:

$$\mathcal{R}_*(\varphi) = \mathcal{R}(\varphi) + \mathcal{R}_0(\varphi) \quad (8)$$

$$= \int_{k_0}^K \frac{1}{K-k_0} \mathbb{E}_{\mathbf{x}^k, \mathbf{y}, \tau} \|\varphi(\mathbf{x}^k, \tau\mathbf{y}, k) - \nabla \log P(\mathbf{x}^k|\tau\mathbf{y})\|_2^2 dk$$

$$+ \int_\delta^K \frac{1}{K-\delta} \mathbb{E}_{\mathbf{x}^k, \mathbf{y}, \tau} \|\varphi(\mathbf{x}^k, \tau\mathbf{y}, k) - \nabla \log P(\mathbf{x}^k|\tau\mathbf{y})\|_2^2 dk$$

which implies that $\mathcal{R}(\varphi) \leq 2\mathcal{R}_*(\varphi)$ with $\varphi(\mathbf{x}^k, \tau\mathbf{y}, k)$ estimating $\nabla \log P(\mathbf{x}^k|\hat{\mathbf{s}}_t, \mathbf{a}_t)$, which is used in the proof of Theorem 2 (see Appendix J). $\hat{\mathbf{x}}^0 = \frac{1}{\sqrt{\bar{\alpha}_\delta}} (\mathbf{x}^\delta - \sqrt{1 - \bar{\alpha}_\delta}\epsilon)$ is the predicted denoised input at step δ . $P(\mathbf{x}^k|\mathbf{x})$ is the Gaussian transition kernel for the forward process of ADM.

To prevent blow-up of score functions, we follow [33], introduce an early-stopping step k_0 , and write \mathcal{R}_* equivalently:

$$\ell(\varphi) := \int_{k_0}^K \frac{1}{K-k_0} \mathbb{E}_{\hat{\mathbf{x}}^0, \mathbf{y}} \left[\mathbb{E}_{\tau, \mathbf{x}^k|\hat{\mathbf{x}}^0} \left[\|\varphi(\mathbf{x}^k, \tau\mathbf{y}, k) - \nabla \log P(\mathbf{x}^k|\hat{\mathbf{x}}^0)\|_2^2 \right] \right] dk + \int_\delta^K \frac{1}{K-\delta} \mathbb{E}_{\mathbf{x}^\delta, \mathbf{y}} \left[\mathbb{E}_{\tau, \mathbf{x}^k|\mathbf{x}^\delta} \left[\|\varphi(\mathbf{x}^k, \tau\mathbf{y}, k) - \nabla \log P(\mathbf{x}^k|\mathbf{x}^\delta)\|_2^2 \right] \right] dk. \quad (9)$$

According to [34, Lemma C.3], (8) differs from (9) by a constant independent of \mathbf{x}^k . ADM is optimized over a mini-batch \mathcal{B} with $|\mathcal{B}| = n$ by minimizing the empirical loss:

$$\hat{\ell}(\varphi) = \sum_{t \in \mathcal{B}} \ell(\mathbf{x}_t, \mathbf{y}_t; \varphi) / n. \quad (10)$$

Here, $\ell(\mathbf{x}_t, \mathbf{y}_t; \varphi)$ represents the loss computed on the training pair $(\mathbf{x}_t, \mathbf{y}_t)$, replacing the expectation on $(\hat{\mathbf{x}}^0, \mathbf{y})$ in (9).

Substituting the generic denoising model φ and its input \mathbf{x}_{t+1}^k in (10) with the observation-denoising and reward-denoising models θ and ϕ (associated with inputs $\tilde{\mathbf{s}}_{t+1}$ and r_{t+1} , respectively), and recalling that $\mathbf{y} = (\hat{\mathbf{s}}_t, \mathbf{a}_t)$, we derive the following objectives for state and reward estimation:

$$\hat{\mathcal{L}}_{\text{State}}(\theta) = \sum_{t \in \mathcal{B}} \ell(\tilde{\mathbf{s}}_{t+1}, \hat{\mathbf{s}}_{t+1}, \mathbf{a}_t; \theta) / n; \quad (11)$$

$$\hat{\mathcal{L}}_{\text{Rew}}(\phi) = \sum_{t \in \mathcal{B}} \ell(r_{t+1}, \hat{\mathbf{s}}_{t+1}, \mathbf{a}_t; \phi) / n. \quad (12)$$

B. Bisimulation Metric

We extend the concept of bisimulation to POMDPs to achieve effective CSR, i.e., estimating $P(\hat{\mathbf{s}}_t | \mathbf{o}_t)$. Based on the Wasserstein metric, a new bisimulation metric is defined:

Definition 6. Given constants $C_r, C_s \in (0, 1)$, for any pair of causal state and observation $\{\hat{\mathbf{s}}_t \in \mathcal{S}_c, \mathbf{o}_t \in \mathcal{O}\}$ of a P^2 OMDP, the bisimulation metric is defined as

$$d(\hat{\mathbf{s}}_t, \mathbf{o}_t) = \max_{\mathbf{a} \in \mathcal{A}} (C_r W_p(d)(P(r_{t+1}|\hat{\mathbf{s}}_t, \mathbf{a}), P(r_{t+1}|\mathbf{o}_t, \mathbf{a})) + C_s W_p(d)(P(\hat{\mathbf{s}}_{t+1}|\hat{\mathbf{s}}_t, \mathbf{a}), P(\hat{\mathbf{s}}_{t+1}|\mathbf{o}_t, \mathbf{a}))). \quad (13)$$

A distance of zero indicates bisimilarity. Combining (5a) with $\hat{F}(\cdot)$ in Definition 4, it follows that the causal state learning objective is equivalent to inferring the conditional distribution $P(\hat{\mathbf{s}}_t | \mathbf{o}_t)$. We employ a recurrent neural network (RNN) $\zeta(\mathbf{o}_t)$ to approximate the noised causal state, i.e., fitting $P(\hat{\mathbf{s}}_t | \mathbf{o}_t)$, which is utilized by ADM to obtain denoised causal state $\hat{\mathbf{s}}_t$. Besides, we here can obtain $\tilde{\mathbf{s}}_{t+1}$ introduced above as $\tilde{\mathbf{s}}_{t+1} = \zeta(\mathbf{o}_{t+1})$. Given Definition 6, we can empirically estimate the CSR by minimizing

$$\hat{\mathcal{L}}_{\text{BS}}(\zeta) = \frac{1}{2} \mathbb{E} [W_d(P(\hat{\mathbf{s}}_{t+1} | \hat{\mathbf{s}}_t, \mathbf{a}_t), \theta(\zeta(\mathbf{o}_t), \mathbf{a}_t))];$$

$$\hat{\mathcal{L}}_{\text{BR}}(\zeta) = \frac{1}{2} \mathbb{E} [W_d(P(r_{t+1} | \hat{\mathbf{s}}_t, \mathbf{a}_t), \phi(\zeta(\mathbf{o}_t), \mathbf{a}_t))].$$

Thus, we implement CSR and assist RL decisions, by iteratively optimizing $\hat{\mathcal{L}}_{\text{State}}(\theta) + \hat{\mathcal{L}}_{\text{BS}}(\zeta)$ and $\hat{\mathcal{L}}_{\text{Rew}}(\phi) + \hat{\mathcal{L}}_{\text{BR}}(\zeta)$.

IV. THEORETICAL GUARANTEE OF CADIFF

This section provides a theoretical guarantee for CaDiff with the value function used to measure the discrepancy between observations and their causal states. Following [27], we begin by imposing a mild light-tail assumption on the initial conditional data distribution as follows.

Assumption 1. For a fixed radius B and a $P^2\text{OMDP}$ \mathcal{M} , define the b -Hölder function $f \in \mathcal{H}^b(\mathbb{R}^{w_x} \times \mathbb{R}^{w_y}, B)$ with $w_y = w_s + w_a$. For $C, C_1 > 0$, we assume $f(\mathbf{x}_{\text{tr}}, \hat{\mathbf{s}}_t, \mathbf{a}_t) \geq C$, $\forall(\mathbf{x}_{\text{tr}}, \hat{\mathbf{s}}_t, \mathbf{a}_t)$, and the true conditional density function yields $P(\mathbf{x}_{\text{tr}} | \hat{\mathbf{s}}_t, \mathbf{a}_t) = \exp(-C_1 \|\mathbf{x}_{\text{tr}}\|_2^2 / 2) \cdot f(\mathbf{x}_{\text{tr}}, \hat{\mathbf{s}}_t, \mathbf{a}_t)$.

As provable tightness implies theoretical guarantees in VFA, the key to bisimulation metrics is their connection to value functions. To generalize the VFA bound, we assume the existence and uniqueness of the p -Wasserstein bisimulation metric for any state pair to measure their similarity, as follows.

Assumption 2 (p -Wasserstein bisimulation metric). For $P^2\text{OMDP}$ \mathcal{M} , any given $C_r, C_s \in (0, 1)$, $C_r + C_s < 1$, any $(\hat{\mathbf{s}}_i, \hat{\mathbf{s}}_j) \in \mathcal{S}_c \times \mathcal{S}_c$, and $p \geq 1$, we assume that the bisimulation metric $d(\hat{\mathbf{s}}_i, \hat{\mathbf{s}}_j)$ in (15) exists and is unique:

$$d(\hat{\mathbf{s}}_i, \hat{\mathbf{s}}_j) = \max_{\mathbf{a} \in \mathcal{A}} (C_r W_p(d)(P(r_{i+1} | \hat{\mathbf{s}}_i, \mathbf{a}), P(r_{i+1} | \hat{\mathbf{s}}_j, \mathbf{a})) + C_s W_p(d)(P(\hat{\mathbf{s}}_{i+1} | \hat{\mathbf{s}}_i, \mathbf{a}), P(\hat{\mathbf{s}}_{j+1} | \hat{\mathbf{s}}_j, \mathbf{a}))). \quad (15)$$

Remark 1. If both policy and environment are deterministic or $p = 1$, Assumption 2 holds.

Proof. See Appendix A. \square

To verify the denoised causal state approximation, we analyze CaDiff in the following four steps, by establishing the upper bound of VFA under the ADM approximation error:

Step 1: p -Wasserstein value difference bound for any state pair: Like the bounds in [35], [36] for policy-independent bisimulation metrics, the bisimulation metric can be bounded: $|V^\pi(\hat{\mathbf{s}}_i) - V^\pi(\hat{\mathbf{s}}_j)| \leq d(\hat{\mathbf{s}}_i, \hat{\mathbf{s}}_j)$ with $d(\hat{\mathbf{s}}_i, \hat{\mathbf{s}}_j)$ defined in Assumption 2, where $V^\pi(\hat{\mathbf{s}}) = \mathbb{E}_\pi[\sum_{i=0}^{\infty} \gamma^i r_{t+i+1} | \mathbf{s}_t = \hat{\mathbf{s}}]$.

Theorem 1 (Value difference bound for p -Wasserstein distance). For the bisimulation metric defined in (15), for any $p \geq 1$, $C_s \in [\gamma, 1)$, $C_r \in (0, 1)$, and $C_r + C_s < 1$, the bisimulation distance between two states provides the bound on the discrepancy in the VFA:

$$C_r |V^\pi(\hat{\mathbf{s}}_i) - V^\pi(\hat{\mathbf{s}}_j)| \leq d(\hat{\mathbf{s}}_i, \hat{\mathbf{s}}_j), \quad \forall(\hat{\mathbf{s}}_i, \hat{\mathbf{s}}_j) \in \mathcal{S}_c \times \mathcal{S}_c. \quad (16)$$

Proof. See Appendix B. \square

As revealed in (16), the bisimulation metric in (15) reflects the upper bound of the value gap.

Step 2: Value difference bound for observation/state pairs: The influence of the model errors on the VFA with the optimal policy-dependent bisimulation distance is as follows.

Theorem 2 (Value difference bound with model errors). For $P^2\text{OMDP}$ \mathcal{M} , let $\zeta : \tilde{\mathcal{O}} \rightarrow \tilde{\mathcal{S}}_c$ be a function mapping observations to noised causal states such that $\zeta(\mathbf{o}_i) = \zeta(\mathbf{o}_j)$ is equivalent to $\hat{d}_\zeta(\tilde{\mathbf{s}}_i, \tilde{\mathbf{s}}_j) = \|\zeta(\mathbf{o}_i) - \zeta(\mathbf{o}_j)\|_q \leq 2\hat{\epsilon}$ for $\tilde{\mathbf{s}}_i = \zeta(\mathbf{o}_i)$ and $\tilde{\mathbf{s}}_j = \zeta(\mathbf{o}_j)$. For $C_r \in (0, 1)$, $C_s \in [\gamma, 1)$, $C_r + C_s < 1$, and $p = 1$, then: $\forall \mathbf{s}_c \in \mathcal{S}_c$,

$$|V^\pi(\mathbf{s}_c) - V^\pi(\hat{F}(\mathbf{o}))| \leq (2\hat{\epsilon} + \mathcal{E}_\zeta + 2C_r \mathcal{E}_\phi / (1 - C_s - C_r) + 2C_s \mathcal{E}_\theta / (1 - C_s - C_r)) / C_r (1 - \gamma),$$

where $\mathcal{E}_\zeta := \|\hat{d}_\zeta - \hat{d}\|_\infty$ is the bisimulation metric learning error, $\mathcal{E}_\phi := W_1(d)(P(r | \mathbf{s}_c, \mathbf{a}), P(r | \hat{F}(\mathbf{o}), \mathbf{a}))$ is the reward approximation error, and $\mathcal{E}_\theta := W_1(d)(P(\mathbf{s}' | \mathbf{s}_c, \mathbf{a}), P(\mathbf{s}' | \hat{F}(\mathbf{o}), \mathbf{a}))$ is the state transition model error. $\hat{\epsilon}$ denotes the aggregation radius in ζ -space. $\hat{d}(\tilde{\mathbf{s}}_i, \tilde{\mathbf{s}}_j)$ denotes the bisimulation metric computed under the estimated environment dynamics, while $\hat{d}_\zeta(\tilde{\mathbf{s}}_i, \tilde{\mathbf{s}}_j)$ represents its approximation derived from ζ .

Proof. See Appendix C. \square

By Theorem 2, we can quantify the upper bound of the value gap under arbitrary model errors. This can be extended to different probability density estimation models to establish specific convergence properties.

Step 3: Distribution estimation under ADM: Since \mathcal{E}_θ and \mathcal{E}_ϕ are based on the same ADM architecture, we define the approximation error of the conditional probability as $\varphi(\mathbf{x}^k, \hat{\mathbf{s}}_t, \mathbf{a}_t, k)$, where \mathbf{x}^k can be replaced by $\hat{\mathbf{s}}_{t+1}$ or r_{t+1} . Under Assumption 1, we measure the ADM's distribution estimation by considering the initialization error, score estimation error, and discretization error, and provide sample complexity bounds for each of these errors using the Wasserstein-1 distance. We utilize an approximation theory for estimating the conditional score with ReLU neural networks (NNs).

Theorem 3 (Approximation error by ADM). Under Assumption 1, for any given $(\mathbf{s}_c^*, \mathbf{a}^*)$, terminal step $K = \frac{2b}{2w_s + w_a + 2b} \log n$, and early-stopping step $k_0 = n^{-\frac{4b}{2w_s + w_a + 2b} - 1}$, the estimated error of the conditional probability of noiseless data is given by

$$\mathbb{E} \left[W_1(P(\hat{\mathbf{x}}^0 | \hat{\mathbf{s}}_t, \mathbf{a}_t), \hat{P}(\mathbf{x}^{k_0} | \hat{\mathbf{s}}_t, \mathbf{a}_t)) \right] = \mathcal{T}(\mathbf{s}_c^*, \mathbf{a}^*) O \left(n^{-\frac{b}{2w_s + w_a + 2b}} (\log n)^{\max(19/2, (b+2)/2)} \right),$$

where b is the degree of smoothness in Hölder norm; w_s and w_a represent the dimensions of state and action, respectively; $\mathcal{T}(\mathbf{s}_c^*, \mathbf{a}^*)$ is the distribution coefficient.

Proof. See Appendix D. \square

As $n \rightarrow \infty$, the distribution estimation measured by the Wasserstein-1 distance converges, i.e.,

$$\mathbb{E}_{\{\mathbf{o}_t, \mathbf{a}_t, r_{t+1}, \mathbf{o}_{t+1}\}} \left[W_1(P(\hat{\mathbf{x}}^0 | \hat{\mathbf{s}}_t, \mathbf{a}_t), \hat{P}(\mathbf{x}^{k_0} | \hat{\mathbf{s}}_t, \mathbf{a}_t)) \right] \rightarrow 0,$$

showing the effective distribution estimation of ADM.

Step 4: Wasserstein value difference bound under ADM: The bisimulation metric learning can be achieved, e.g., by an RNN, whose convergence rate of \mathcal{E}_ζ is $\mathcal{O} \left(n^{-\frac{2p_R}{2p_R + w_s + 1}} (\log n)^6 \right)$ with the model size p_R [37]. Substituting the approximation error in Theorem 3 with the respective error terms, \mathcal{E}_ϕ and

\mathcal{E}_θ , introduced in Theorems 2, we establish the theoretical guarantee of CaDiff in P²OMDPs, as follows.

Theorem 4 (Value difference bound with ADM). *Consider the conditions in Theorems 2 and 3. Let $c_b = \max\{\frac{19}{2}, \frac{b+2}{2}\}$. $\forall s \in \mathcal{S}$,*

$$\begin{aligned} \mathbb{E} \left[\left| V^\pi(s_c) - V^\pi(\hat{F}(\mathbf{o})) \right| \right] &\leq 2\hat{\epsilon} \\ &+ \frac{1}{C_r(1-\gamma)} \left(\mathcal{O} \left(n^{-2p_R/(2p_R+w_s+1)} (\log n)^6 \right) \right) \\ &+ \frac{2C_r + 2C_s}{1 - C_s - C_r} \mathcal{T}(s_c^*, \mathbf{a}^*) \mathcal{O} \left(n^{-b/(2w_s+w_a+2b)} (\log n)^{c_b} \right). \end{aligned} \quad (17)$$

As $n \rightarrow \infty$, the approximate value function for the estimated causal state $V^\pi(\hat{F}(\mathbf{o}))$ in (17) converges to within $2\hat{\epsilon}$ -neighborhood of the ground-truth causal state $V^\pi(s_c)$. The parameters (C_r, C_s) ensure a trade-off between the reward approximation error and the state transition model error, while $\frac{1}{C_r(1-\gamma)}$ and $\frac{2C_r+2C_s}{1-C_s-C_r}$ balance the approximation error of the bisimulation and that of the noisy distribution.

Computational cost: We evaluate the additional computational cost of CaDiff on top of RL algorithms. From [38], the computational cost of a DM is $\tilde{\mathcal{O}}(\text{poly log } d_i)$, where d_i is the dimension of the input data. The loss function of ADM includes two terms to be computed, i.e., (10), thereby doubling the computational cost of a standard DM. The additional computational cost of CSR is $\tilde{\mathcal{O}}(\text{poly log max}\{|\mathcal{A}|, |\mathcal{O}|\})$ in CaDiff, as empirically evaluated in Section V-4.

V. EXPERIMENTS

To evaluate CaDiff in classical control tasks with high degrees of freedom (DoFs), we consider Roboschool tasks under standard POMDPs [39]. There are six environments, i.e., {Hopper, Ant, Walker}-{P, V}, where “-P” stands for observing positions and angles only, and “-V” stands for observing velocities only. In the no-velocities (i.e., “-P”) settings, velocity features are excluded from the raw observations; in the velocities-only (i.e., “-V”) settings, the observations contain only velocity-related information. Details for each environment are summarized in Table I with a maximum of 1,000 steps. In all experiments, both the rewards and observations are perturbed by zero-mean Gaussian noise, whose variance is scaled by a noise scale to control the perturbation intensity. Unless otherwise specified, the noise intensity is set to $\delta = 2$ to evaluate the impact of the noise. Since CaDiff can accommodate any RL algorithm, we consider SAC, a typical RL algorithm. We evaluate all experiments with 600,000 iterations and smooth each return. The hyperparameters are summarized in Table II.

1) *Comparison with Baselines:* Compared to classical SAC, DMBP [8] (only denoising), and DBC [11] (only considering bisimulation), we demonstrate the effectiveness and scalability of CaDiff. In Fig. 2, CaDiff demonstrates superior performance across six environments. Compared to DMBP in Walker-V or DBC in Hopper-P, CaDiff exhibits superior generalization capabilities. Notably, CaDiff improves returns by at least 14.18%, 29.42%, and 136.63% across the six environments when compared to SAC, DMBP, and DBC,

TABLE I
INFORMATION OF ENVIRONMENTS IN THIS PAPER

Name	Dimension of observation space	DoF
RoboschoolAnt	28	8
RoboschoolAnt-V	11	8
RoboschoolAnt-P	17	8
RoboschoolHopper	15	3
RoboschoolHopper-V	6	3
RoboschoolHopper-P	9	3
RoboschoolWalker2d	22	6
RoboschoolWalker2d-V	9	6
RoboschoolWalker2d-P	13	6

TABLE II
HYPERPARAMETERS FOR TASKS

Description	Value
Number of training iterates	600
Size of replay memory	10^6
Number of samples for each update	64
Discount factor	0.99
Fraction of updating the target network per gradient step	0.005
Learning rate for the policy and value networks	0.0003
Learning rate for the entropy coefficient in SAC	0.0003
Target entropy in SAC	0.2
Learning rate of the asynchronous diffusion model	0.0003
Learning rate of the bisimulation metric learning	0.0003
Network for the asynchronous diffusion model	UNet
Total diffusion step	500
Beta schedule	linear
Noise intensity of observation and reward	2

respectively. CaDiff achieves better performance in the early stages of training in five out of six environments.

2) *Ablation Study:* We proceed to disable individual modules of CaDiff: bisimulation, reward denoising, and observation denoising. Fig. 3 presents the ablation study of CaDiff across six environments. By comparing these three cases with our approach, it is evident that both bisimulation and ADM contribute to the return. In most environments, reward denoising is much less effective than state denoising. This can be attributed to the higher observation dimension compared to the reward, resulting in a greater impact of its noise. Additionally, the environments of Hopper-V and Walker-P exhibit higher sensitivity to noise (see Table III).

3) *Influence on Key Parameters:* We evaluate CaDiff across three noise scales with varying intensities in six environments in Table III. Bold numbers indicate the optimal results for each environment and noise scale. The conclusion drawn across the six environments is that for a noise scale of 0.1, the optimal noise intensity is $\delta = 1$; for a noise scale of 0.5, the optimal noise intensity is $\delta = 2$. When the noise scale increases to 1, the optimal noise intensity becomes unstable and fluctuates between 1 and 3, indicating that a larger noise intensity may be required to ensure reliable estimation under higher noise scales. As the noise scale increases from 0.1 to 0.5, half of the environments exhibit relatively stable returns. When the noise scale rises from 0.5 to 1, the returns of CaDiff across all six environments show no significant change. In this sense, CaDiff can maintain stable performance under high noise intensity.

4) *Computational Cost:* We provide a quantitative analysis of the additional computational cost introduced by our denoising CSR using the FLOPs metric. Experiments are conducted on PyTorch 2.0.0 with an NVIDIA RTX 4090 24GB GPU, as shown in Table IV. We also report the average runtime over 200 iterations across six environments. The runtime varies

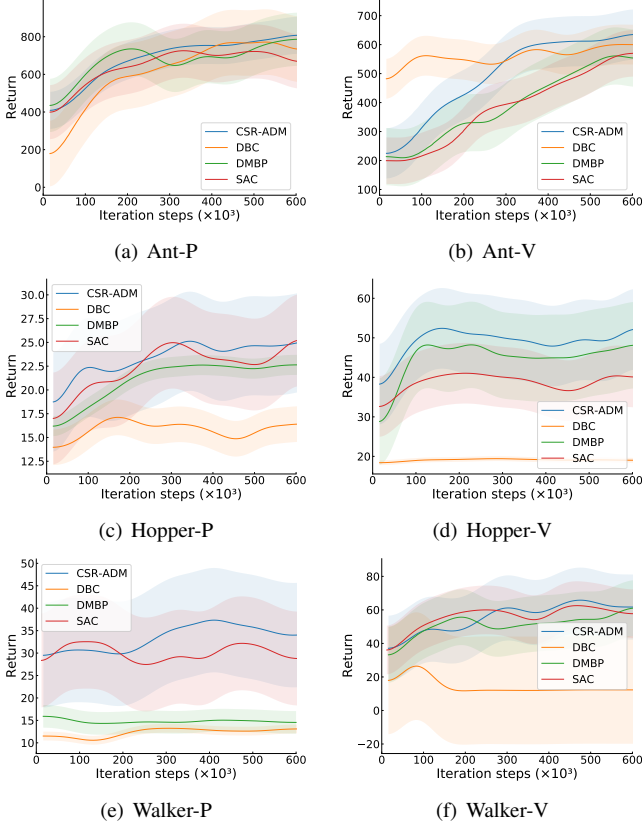


Fig. 2. Comparison of CaDiff and baselines on six environments.

TABLE III

RETURNS OF NOISE INTENSITIES WITH VARIOUS NOISE SCALES.

Noise scale	δ	Ant-P	Ant-V	Hopper-P	Hopper-V	Walker-P	Walker-V
0.1	1	790.8	573.8	214	183	285.1	65.44
	2	764.2	499.1	153.3	161	221.3	52.68
	3	694	466	122.4	128.7	215.4	58.05
0.5	1	727.7	465.4	23.87	45.58	31.04	58.15
	2	789.3	615.4	24.18	50.17	34.01	65.24
	3	670.9	560.3	21.94	43.3	31.23	61.03
1	1	569.2	538.2	24.93	45.26	35.25	50.45
	2	597.3	533.8	26.2	48.16	35.8	53.36
	3	648.3	528.4	25.53	48.96	33.3	62.26

around 200 ms per update on average. Compared to SAC, the complexity of our method is increased by less than 7 GFLOPs, lower than the typical overhead of DMs; see [40].

VI. CONCLUSION

This paper introduces *CaDiff* that effectively addresses the challenges posed by high-dimensional and noisy inputs to RL in P²OMDPs. Integrating the new ADM for denoising both rewards and observations with a new bisimulation metric, *CaDiff* captures essential CSRs, which are crucial for decision-making tasks. Our analysis provides rigorous guarantees for the approximation of value functions between noisy observation spaces and causal state spaces. Experiments corroborate *CaDiff*'s superiority, enhancing the performance and robustness of RL under various noise conditions. This research lays the groundwork for studies on CSR in noisy environments.

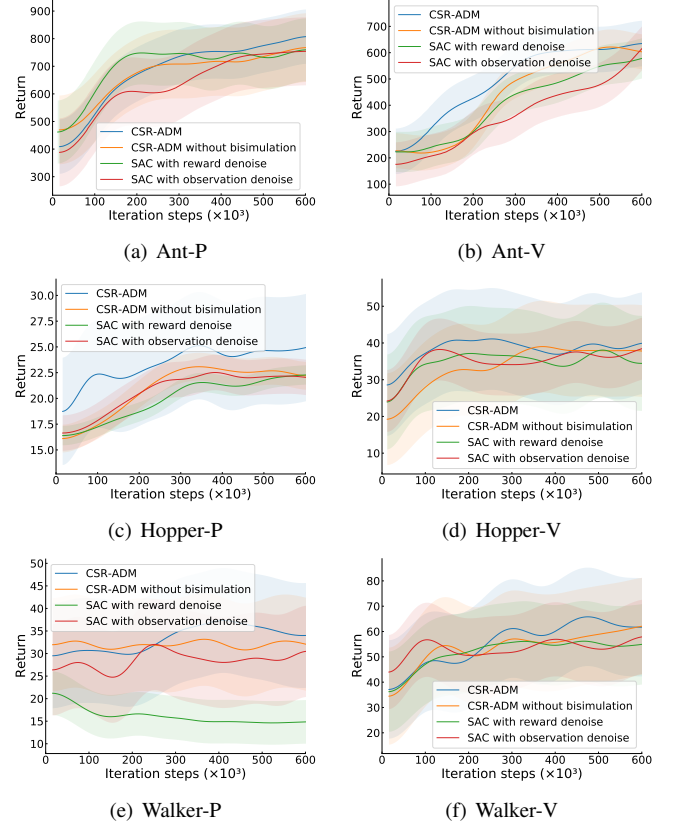


Fig. 3. Ablation studies of CaDiff on six environments.

TABLE IV

COMPUTATIONAL COST IN TERMS OF FLOPS AND RUNTIME (MS).

		Ant	Hopper	Walker
FLOPs on “-P”	GFLOPs of ϕ	3.3354	3.3350	3.3352
	GFLOPs of θ	3.3365	3.3355	3.3360
	GFLOPs of ζ	0.2785	0.1474	0.2129
FLOPs on “-V”	GFLOPs of ϕ	3.3352	3.3349	3.3351
	GFLOPs of θ	3.3359	3.3352	3.3356
	GFLOPs of ζ	0.1802	0.9830	0.1474
Runtime on “-P”	CaDiff	208.95	219.06	221.69
	SAC	25.03	25.06	24.35
	DMBP	86.64	87.67	87.11
Runtime on “-V”	DBC	40.29	41.03	41.27
	CaDiff	209.09	211.93	219.99
	SAC	24.60	24.74	24.17
	DMBP	87.04	88.26	87.56
	DBC	41.95	41.41	41.09

APPENDIX

A. Proof of Remark 1

We first prove that the update $d(\hat{s}_i, \hat{s}_j)$ satisfies the contraction property. Applying the Banach fixed-point theorem then ensures the existence and uniqueness of the resulting metric. Start with $p = 1$ under the Cauchy–Schwarz inequality as:

$$\begin{aligned}
 & d(\hat{s}_i, \hat{s}_j) - d'(\hat{s}_i, \hat{s}_j) \\
 & \leq \max_{\mathbf{a} \in \mathcal{A}} \left(C_r W_1 \|d - d'\|_\infty (P(r_{i+1} | \hat{s}_i, \mathbf{a}), P(r_{j+1} | \hat{s}_j, \mathbf{a})) \right. \\
 & \quad \left. + C_s W_1 \|d - d'\|_\infty (P(s' | \hat{s}_i, \mathbf{a}), P(s' | \hat{s}_j, \mathbf{a})) \right) \\
 & \leq (C_r + C_s) \|d - d'\|_\infty, \quad \forall (\hat{s}_i, \hat{s}_j) \in \mathcal{S}_c \times \mathcal{S}_c. \quad (18)
 \end{aligned}$$

For $C_r + C_s \in [0, 1)$, the Banach fixed-point theorem [41] guarantees the existence and uniqueness of the fixed point.

We turn to the deterministic setting, where both P and π are deterministic, implying P being delta distribution.

$$\begin{aligned}
& C_r |V^{(t+1)}(\hat{\mathbf{s}}_i) - V^{(t+1)}(\hat{\mathbf{s}}_j)| \\
& \leq C_r \left| \max_{\mathbf{a} \in \mathcal{A}} \left(\int_{r \in \mathcal{R}} r(\hat{\mathbf{s}}_i, \mathbf{a}) P(r_{i+1} | \hat{\mathbf{s}}_i, \mathbf{a}) dr - \int_{r \in \mathcal{R}} r(\hat{\mathbf{s}}_j, \mathbf{a}) P(r_{j+1} | \hat{\mathbf{s}}_j, \mathbf{a}) dr + \gamma \int_{\mathbf{s}' \in \mathcal{S}} (P(\mathbf{s}' | \hat{\mathbf{s}}_i, \mathbf{a}) - P(\mathbf{s}' | \hat{\mathbf{s}}_j, \mathbf{a})) V^{(t)}(\mathbf{s}') d\mathbf{s}' \right) \right| \\
& \leq C_r \max_{\mathbf{a} \in \mathcal{A}} \left| \int_{r \in \mathcal{R}} r(\hat{\mathbf{s}}_i, \mathbf{a}) P(r_{i+1} | \hat{\mathbf{s}}_i, \mathbf{a}) dr - \int_{r \in \mathcal{R}} r(\hat{\mathbf{s}}_j, \mathbf{a}) P(r_{j+1} | \hat{\mathbf{s}}_j, \mathbf{a}) dr \right| + C_s \gamma \max_{\mathbf{a} \in \mathcal{A}} \left| \int_{\mathbf{s}' \in \mathcal{S}} (P(\mathbf{s}' | \hat{\mathbf{s}}_i, \mathbf{a}) - P(\mathbf{s}' | \hat{\mathbf{s}}_j, \mathbf{a})) \frac{C_r \gamma}{C_s} V^{(t)}(\mathbf{s}') d\mathbf{s}' \right| \\
& C_r |V^{(t+1)}(\hat{\mathbf{s}}_i) - V^{(t+1)}(\hat{\mathbf{s}}_j)| \leq C_r \max_{\mathbf{a} \in \mathcal{A}} \left(W_1(d^{(t)})(P(r_{i+1} | \hat{\mathbf{s}}_i, \mathbf{a}), P(r_{j+1} | \hat{\mathbf{s}}_j, \mathbf{a})) \right) + C_s \max_{\mathbf{a} \in \mathcal{A}} \left(W_1(d^{(t)})(P(\mathbf{s}' | \hat{\mathbf{s}}_i, \mathbf{a}), P(\mathbf{s}' | \hat{\mathbf{s}}_j, \mathbf{a})) \right) \\
& \leq C_r \max_{\mathbf{a} \in \mathcal{A}} \left(W_p(d^{(t)})(P(r_{i+1} | \hat{\mathbf{s}}_i, \mathbf{a}), P(r_{j+1} | \hat{\mathbf{s}}_j, \mathbf{a})) \right) + C_s \max_{\mathbf{a} \in \mathcal{A}} \left(W_p(d^{(t)})(P(\mathbf{s}' | \hat{\mathbf{s}}_i, \mathbf{a}), P(\mathbf{s}' | \hat{\mathbf{s}}_j, \mathbf{a})) \right) = d^{(t+1)}, \quad (23)
\end{aligned}$$

As noted in Definition 1, the Wasserstein distance satisfies $W_p(d)(\Delta(\hat{\mathbf{s}}_i), \Delta(\hat{\mathbf{s}}_j)) = d(\mathbf{s}_i, \mathbf{s}_j)$ for point masses, where $\Delta(\cdot)$ denotes the Dirac delta function. Under the fact that

$$\begin{aligned}
d(\hat{\mathbf{s}}_i, \hat{\mathbf{s}}_j) - d'(\hat{\mathbf{s}}_i, \hat{\mathbf{s}}_j) &= \max_{\mathbf{a} \in \mathcal{A}} \left(C_r (d(r_{i'}, r_{j'}) - d'(r_{i'}, r_{j'})) \right. \\
&\quad \left. + C_s (d(r_{i'}, r_{j'}) - d'(r_{i'}, r_{j'})) \right) \leq (C_r + C_s) \|d - d'\|_\infty,
\end{aligned}$$

the convergence of the update $d^{(n+1)}(\hat{\mathbf{s}}_i, \hat{\mathbf{s}}_j)$ from $d^{(n)}(\hat{\mathbf{s}}_i, \hat{\mathbf{s}}_j)$ is ensured when the underlying POMDP is finite, $\forall \hat{\mathbf{s}}_i, \hat{\mathbf{s}}_j$.

B. Proof of Theorem 1

We prove (16) by induction with the update rules:

$$\begin{aligned}
V^{(t+1)}(\hat{\mathbf{s}}_i) &= \max_{\mathbf{a} \in \mathcal{A}} \left(\int_{r \in \mathcal{R}} r(\hat{\mathbf{s}}_i, \mathbf{a}) P(r_{i+1} | \hat{\mathbf{s}}_i, \mathbf{a}) dr \right. \\
&\quad \left. + \gamma \int_{\mathbf{s}' \in \mathcal{S}} P(\mathbf{s}' | \hat{\mathbf{s}}_i, \mathbf{a}) V^{(t)}(\mathbf{s}') d\mathbf{s}' \right) \quad (19)
\end{aligned}$$

$$\begin{aligned}
d^{(t+1)}(\hat{\mathbf{s}}_i, \hat{\mathbf{s}}_j) &= \max_{\mathbf{a} \in \mathcal{A}} (C_r W_p(d^{(t)})(P(r_{i+1} | \hat{\mathbf{s}}_i, \mathbf{a}), P(r_{j+1} | \hat{\mathbf{s}}_j, \mathbf{a})) \\
&\quad + C_s W_p(d^{(t)})(P(\mathbf{s}' | \hat{\mathbf{s}}_i, \mathbf{a}), P(\mathbf{s}' | \hat{\mathbf{s}}_j, \mathbf{a}))). \quad (20)
\end{aligned}$$

We proceed to demonstrate that, $\forall t \in \mathbb{N}$,

$$C_r |V^{(t)}(\hat{\mathbf{s}}_i) - V^{(t)}(\hat{\mathbf{s}}_j)| \leq d^{(t)}(\hat{\mathbf{s}}_i, \hat{\mathbf{s}}_j), \forall (\hat{\mathbf{s}}_i, \hat{\mathbf{s}}_j) \in \mathcal{S}_c \times \mathcal{S}_c. \quad (21)$$

Then, (16) holds as $t \rightarrow \infty$. With mathematical induction, the base case $t = 0$ satisfies because

$$|V^{(0)}(\hat{\mathbf{s}}_i) - V^{(0)}(\hat{\mathbf{s}}_j)| = d^{(0)}(\hat{\mathbf{s}}_i, \hat{\mathbf{s}}_j) = 0, \forall (\hat{\mathbf{s}}_i, \hat{\mathbf{s}}_j) \in \mathcal{S}_c \times \mathcal{S}_c.$$

Assume (21) holds $\forall t$. In the case of $t + 1$, we have (22) under triangle inequality. By the induction hypothesis, the function $C_r V^{(t)}(\hat{\mathbf{s}})$ is 1-Lipschitz w.r.t. the metric $d^{(t)}$, that is, $C_r V^{(t)}(\hat{\mathbf{s}}) \in \text{Lip}_{1, d^{(t)}}$. Since $\gamma \leq C_s$ by assumption, $\frac{C_r \gamma}{C_s} V^{(t)}(\hat{\mathbf{s}})$ is 1-Lipschitz. Under the assumption of $r(\hat{\mathbf{s}}, \mathbf{a}) \in \text{Lip}_{1, d^{(t)}}$, the dual form of the W_1 metric in (2) leads to (23), where the second inequality holds due to Lemma 1.

C. Proof of Theorem 2

We first introduce two useful lemmas.

Lemma 3 (Bound for convergence). *Let \mathcal{S}_c be compact. If the support $\mathcal{S}'_c = \text{supp}(\hat{P}) \subset \mathcal{S}_c$ of the fitted dynamics \hat{P} is closed, (15) admits a unique bounded bisimulation metric \hat{d} :*

$$\text{supp}(\hat{P}) \subseteq \mathcal{S}_c \Rightarrow \text{diam}(\mathcal{S}_c; \hat{d}) \leq C_r (r_{\max} - r_{\min}) / (1 - C_s).$$

Proof. See Appendix E. \square

Lemma 4 (Bisimulation distance approximation error). *Define $C_r \geq 0$ and $C_s \in [0, 1)$. Suppose $\text{supp}(\hat{P}) \subseteq \mathcal{S}_c$ and $1 -$*

$(C_r + C_s)a_p > 0$. With $a_p = 2^{(p-1)/p}$ and $\text{diam}(\mathcal{S}_c; d) \leq \frac{C_r}{1-C_s}(r_{\max} - r_{\min})$, based on Lemma 3, there is

$$\begin{aligned}
\|d - \hat{d}\|_\infty &\leq [(C_r + C_s)(a_p - 1)\text{diam}(\mathcal{S}_c; d) \\
&\quad + 2C_r \mathcal{E}_\phi + 2C_s \mathcal{E}_\theta] / [1 - (C_r + C_s)a_p]. \quad (24)
\end{aligned}$$

Proof. See Appendix F. \square

If $p = 1$, there is $a_p = a_1 = 1$. Based on Lemma 4, we obtain the following Corollary.

Corollary 1 (Bisimulation distance approximation error for $p = 1$). *On the remaining conditions in Lemma 4, for $p = 1$,*

$$\|d - \hat{d}\|_\infty \leq \frac{2C_r}{1 - C_r - C_s} \mathcal{E}_\phi + \frac{2C_s}{1 - C_r - C_s} \mathcal{E}_\theta. \quad (25)$$

Corollary 1 establishes a bound on the deviation between the true bisimulation distance and its optimal *approximate* counterpart, reflecting the achievable distance under encoder and ADM approximation errors. We express the VFA error w.r.t. \hat{d}_ζ (not \hat{d}), incorporating the effect of encoder and ADM. Using Corollary 1 and the definition of bisimulation encoder,

$$\begin{aligned}
\|d - \hat{d}_\zeta\|_\infty &\leq \|d - \hat{d}\|_\infty + \|\hat{d}_\zeta - \hat{d}\|_\infty \\
&\leq \frac{2C_r}{1 - C_r - C_s} \mathcal{E}_\phi + \frac{2C_s}{1 - C_r - C_s} \mathcal{E}_\theta + \mathcal{E}_\zeta. \quad (26)
\end{aligned}$$

Once d relates to VFA, a similar relationship can be established for \hat{d}_ζ as a function of the model approximation error.

Let $\hat{\epsilon}$ denote the aggregation radius in ζ -space, such that the \hat{d}_ζ -diameter of each equivalence class (or partition subset) is bounded by $2\hat{\epsilon}$. Thus, $\sup_{\mathbf{o}_i, \mathbf{o}_j \in \mathcal{O}} \|\zeta(\mathbf{o}_i) - \zeta(\mathbf{o}_j)\|_q \leq 2\hat{\epsilon}$. Note that $\hat{\epsilon}$ provides an upper bound on the maximum diameter of the partition cells w.r.t. the learned distance induced by ζ , not the true bisimulation distance.

Lemma 5 (Value difference bound with causal state). *Let $\zeta : \mathcal{O} \rightarrow \hat{\mathcal{S}}_c$ be a function mapping denoised observations to causal states such that $\zeta(\mathbf{o}_i) = \zeta(\mathbf{o}_j)$ is equivalent to $d(\hat{\mathbf{s}}_i, \hat{\mathbf{s}}_j) \leq 2\epsilon$. For $C_r, C_s \in [0, 1)$ and $C_r + C_s < 1$:*

$$|V^\pi(\mathbf{s}_c) - V^\pi(\hat{F}(\mathbf{o}))| \leq 2\epsilon / [C_r(1 - \gamma)], \forall \mathbf{s}_c \in \mathcal{S}_c. \quad (27)$$

Proof. See Appendix G. \square

From Lemma 5, it readily follows that

$$\begin{aligned}
(1 - \gamma)|V(\mathbf{s}_c) - V(\hat{F}(\mathbf{o}))| &\leq \frac{C_r^{-1}}{\xi(\hat{F}(\mathbf{o}))} \int_{\mathbf{z} \in \hat{F}(\mathbf{o})} d(\mathbf{s}_c, \mathbf{z}) d\xi(\mathbf{z}) \\
&\leq \frac{C_r^{-1}}{\xi(\hat{F}(\mathbf{o}))} \int_{\mathbf{z} \in \hat{F}(\mathbf{o})} \hat{d}_\zeta(\mathbf{s}_c, \mathbf{z}) + |d(\mathbf{s}_c, \mathbf{z}) - \hat{d}_\zeta(\mathbf{s}_c, \mathbf{z})|_\infty d\xi(\mathbf{z}) \\
&\leq \frac{1}{C_r} \left(2\hat{\epsilon} + \mathcal{E}_\zeta + \frac{2C_r}{1 - C_r - C_s} \mathcal{E}_\phi + \frac{2C_s}{1 - C_r - C_s} \mathcal{E}_\theta \right),
\end{aligned}$$

where the last inequality is due to (26). Theorem 2 is proved.

$$\begin{aligned}
W_1(P'(\mathbf{x}^{k_0}|\mathbf{y}), \hat{P}(\mathbf{x}^{k_0}|\mathbf{y})) &\lesssim \sqrt{\int_{k_0}^K \frac{1}{2} \int_{\mathbf{x}^k} P(\mathbf{x}^k|\mathbf{s}_c^*, \mathbf{a}^*) \|\varphi(\mathbf{x}^k, \mathbf{s}_c^*, \mathbf{a}^*, k) - \nabla \log P(\mathbf{x}^k|\mathbf{s}_c^*, \mathbf{a}^*)\|^2 d\mathbf{x} dk} \\
&= \sqrt{\frac{\int_{k_0}^K \mathbb{E}_{\mathbf{x}^k} [\|\varphi(\mathbf{x}^k, \mathbf{s}_c^*, \mathbf{a}^*, k) - \nabla \log P(\mathbf{x}^k|\mathbf{s}_c^*, \mathbf{a}^*)\|^2] dk}{\int_{k_0}^K \mathbb{E}_{\mathbf{x}^k, \mathbf{s}, \mathbf{a}} [\|\varphi(\mathbf{x}^k, \mathbf{s}, \mathbf{a}, k) - \nabla \log P(\mathbf{x}^k|\mathbf{s}, \mathbf{a})\|^2] dk}} \cdot \sqrt{\frac{K}{2}} \mathcal{R}(\varphi) \leq \mathcal{T}(\mathbf{s}_c^*, \mathbf{a}^*) \sqrt{\frac{K}{2}} \mathcal{R}(\varphi).
\end{aligned} \tag{32}$$

D. Proof of Theorem 3

Notice that we have the following decomposition:

$$\begin{aligned}
W_1(P(\mathbf{x}|\mathbf{y}), \hat{P}(\mathbf{x}^{k_0}|\mathbf{y})) &\leq W_1(P(\mathbf{x}|\mathbf{y}), P(\mathbf{x}^{k_0}|\mathbf{y})) \\
&+ W_1(P(\mathbf{x}^{k_0}|\mathbf{y}), P'(\mathbf{x}^{k_0}|\mathbf{y})) + W_1(P'(\mathbf{x}^{k_0}|\mathbf{y}), \hat{P}(\mathbf{x}^{k_0}|\mathbf{y})),
\end{aligned} \tag{28}$$

where $W_1(P(\mathbf{x}|\mathbf{y}), P(\mathbf{x}^{k_0}|\mathbf{y}))$ follows the correspondence between the forward and backward processes; $W_1(P(\mathbf{x}^{k_0}|\mathbf{y}), P'(\mathbf{x}^{k_0}|\mathbf{y}))$ follows the definitions of \mathbf{x} and \mathbf{x}' (with the only difference in initial distribution), with the latter being the result obtained by the true distribution.

We use another backward process as a transition term between \mathbf{x}'_k and $\bar{\mathbf{x}}'_k$, which is defined as: with $\bar{\mathbf{x}}'_0 \sim \mathcal{N}(0, I)$,

$$d\bar{\mathbf{x}}'_k = [0.5\bar{\mathbf{x}}'_k + \nabla \log P_{K-k}(\bar{\mathbf{x}}'_k|\mathbf{y})] dk + d\hat{\mathbf{w}}_k. \tag{29}$$

Let $P'_{K-k}(\cdot|\mathbf{y})$ denote the conditional distribution of $\bar{\mathbf{x}}'_k$ on \mathbf{y} . We bound the three terms on the RHS of (28), as follows.

Bound $W_1(P(\mathbf{x}|\mathbf{y}), P(\mathbf{x}^{k_0}|\mathbf{y}))$: Let $X \sim P(\mathbf{x}|\mathbf{y})$ and $Z \sim \mathcal{N}(0, I)$. Then,

$$\begin{aligned}
W_1(P(\mathbf{x}|\mathbf{y}), P(\mathbf{x}^{k_0}|\mathbf{y})) &\leq \mathbb{E}[\|X - \sqrt{\alpha_{k_0}}X + \sigma_{k_0}Z\|] \\
&\leq (1 - \sqrt{\alpha_{k_0}})\mathbb{E}[\|X\|] + \sigma_{k_0}\mathbb{E}[\|Z\|] \\
&\leq (1 - \sqrt{\alpha_{k_0}})\sqrt{d} + \sigma_{k_0}\sqrt{d} \lesssim \sqrt{k_0},
\end{aligned} \tag{30}$$

where the last holds since $\sigma_k/\sqrt{\alpha_k} = \mathcal{O}(\sqrt{k})$ if $k = o(1)$.

Bound $W_1(P(\mathbf{x}^{k_0}|\mathbf{y}), P'(\mathbf{x}^{k_0}|\mathbf{y}))$: Because $\bar{\mathbf{x}}'_k$ and $\bar{\mathbf{x}}_k$ evolve under an identical backward stochastic differential equality (SDE) while differing only in their initial distributions, following [42, Lemma 2], we have

$$\begin{aligned}
W_1(P(\mathbf{x}^{k_0}|\mathbf{y}), P'(\mathbf{x}^{k_0}|\mathbf{y})) &\lesssim \text{TV}(P(\mathbf{x}^{k_0}|\mathbf{y}), P'(\mathbf{x}^{k_0}|\mathbf{y})) \\
&\lesssim \sqrt{\text{KL}(P(\mathbf{x}^{k_0}|\mathbf{y})||\mathcal{N}(0, I))} \\
&\lesssim \sqrt{\text{KL}(P(\mathbf{x}|\mathbf{y})||\mathcal{N}(0, I))} \exp(-K) \lesssim \exp(-K).
\end{aligned} \tag{31}$$

Bound $W_1(P'(\mathbf{x}^{k_0}|\mathbf{y}), \hat{P}(\mathbf{x}^{k_0}|\mathbf{y}))$: Although Assumption 1 does not ensure Novikov's condition according to [43], Girsanov's theorem bounds the KL divergence between any two distributions produced from the same SDE, provided the score estimation error possesses a bounded second moment and the KL divergence w.r.t. the standard Gaussian remains finite.

According to [27, Lemma D.4], we obtain

$$\begin{aligned}
W_1(P'(\mathbf{x}^{k_0}|\mathbf{y}), \hat{P}(\mathbf{x}^{k_0}|\mathbf{y})) &\lesssim \text{TV}(P'(\mathbf{x}^{k_0}|\mathbf{y}), \hat{P}(\mathbf{x}^{k_0}|\mathbf{y})) \lesssim \sqrt{\text{KL}(P'(\mathbf{x}^{k_0}|\mathbf{y}), \hat{P}(\mathbf{x}^{k_0}|\mathbf{y}))} \\
&\lesssim \sqrt{\int_{k_0}^K \frac{1}{2} \int_{\mathbf{x}^k} P_k(\mathbf{x}^k|\mathbf{y}) \|\varphi(\mathbf{x}^k, \mathbf{y}, k) - \nabla \log P(\mathbf{x}^k|\mathbf{y})\|^2 d\mathbf{x} dk}.
\end{aligned}$$

For a state-action pair $\mathbf{y}^* = (\mathbf{s}_c^*, \mathbf{a}^*)$, the estimated conditional distribution $P(\mathbf{x}^{k_0}|\mathbf{s}_c^*, \mathbf{a}^*)$ is obtained via the reverse process of ADM, arriving at (32). Besides, the distribution coefficient $\mathcal{T}(\mathbf{s}_c^*, \mathbf{a}^*)$ is aligned with the concentrability coefficient, i.e., L_∞ density ratio in RL [44]. Owing to the smoothing property of the score network \mathcal{F} that mitigates discrepancies between

$(\mathbf{s}_c^*, \mathbf{a}^*)$ and the training data, $\mathcal{T}(\mathbf{s}_c^*, \mathbf{a}^*)$ is persistently lower than the standard concentrability coefficient.

We investigate the theoretical guarantees under the case of approximating the conditional score with a ReLU NN. We derive the bounded covering number of ReLU NN functions by defining a truncated loss function $\ell^{\text{tr}}(\mathbf{x}, \mathbf{y}; \varphi)$ as

$$\ell^{\text{tr}}(\mathbf{x}, \mathbf{y}; \varphi) := \ell(\mathbf{x}, \mathbf{y}; \varphi) \mathbb{I} \{ \|\mathbf{x}\|_\infty \leq R \}.$$

Following this, we define the truncated domain of the score function as $\mathcal{D} = [-R, R]^{w_x} \times \mathbb{R}^{w_y} \cup \{\emptyset\}$, and the associated truncated loss function can be written as

$$\mathcal{S}(R) = \{ \ell(\cdot, \cdot; \varphi) : \mathcal{D} \rightarrow \mathbb{R} | \mathbf{s} \in \mathcal{F} \}. \tag{33}$$

To derive the approximation guarantee with statistical theory, the loss function class's covering number $\mathcal{S}(R)$ is defined:

Definition 7. Let $\mathcal{N}(\varrho, \mathcal{F}, \|\cdot\|)$ denote the ϱ -covering number of the function class \mathcal{F} under the norm $\|\cdot\|$, that is,

$$\begin{aligned}
\mathcal{N}(\varrho, \mathcal{F}, \|\cdot\|) &= \min \{ N : \exists \{f_t\}_{t \in \mathcal{B}} \subseteq \mathcal{F}, \\
&\text{s.t. } \forall f \in \mathcal{F}, \exists t \in [N], \|f_t - f\| \leq \varrho \}.
\end{aligned}$$

We present the covering number associated with $\mathcal{S}(R)$ as:

Lemma 6. For any $\varrho > 0$, under the condition $\|\mathbf{x}\|_\infty \leq R$, the ϱ -covering number of $\mathcal{S}(R)$ under $\|\cdot\|_{L_\infty \mathcal{D}}$ is bounded as

$$\mathcal{N}(\varrho, \mathcal{S}(R), \|\cdot\|_{L_\infty \mathcal{D}}) \lesssim \left(\frac{2L^2(W \max(R, K) + 2)\kappa^L W^{L+1} \log N}{\varrho} \right)^{2P},$$

where the norm $\|\cdot\|_{L_\infty \mathcal{D}}$ is given by

$$\|f(\cdot, \cdot)\|_{L_\infty \mathcal{D}} = \max_{\mathbf{x} \in [-R, R]^{w_x}, \mathbf{y} \in \mathbb{R}^{w_y} \cup \{\emptyset\}} |f(\mathbf{x}, \mathbf{y})|.$$

Proof. See Appendix H. \square

Following from [27, Thm 3.4] established upon [27, Assumption 3.1], we have the key Lemmas as follows.

Lemma 7. Under Assumption 1, for positive constant C_α and large enough N , by setting the terminal step $K = C_\alpha \log N$, $\mathbf{s} \in \mathcal{F}(M_t, W, \kappa, L, P)$ exists and satisfies that, for $\mathbf{y} \in \mathbb{R}^{w_y}$ and $k \in [0, K]$, one has

$$\begin{aligned}
&\int_{\mathbf{x}^{k_1}} \|\zeta(\mathbf{x}^{k_1}, \mathbf{y}, k_1) - \nabla \log P_{k_1}(\mathbf{x}^{k_1}|\mathbf{y})\|_2^2 \cdot P_{k_1}(\mathbf{x}^{k_1}|\mathbf{y}) d\mathbf{x}^{k_1} \\
&+ \int_{\mathbf{x}^{k_2}} \|\zeta(\mathbf{x}^{k_2}, \mathbf{y}, k_2) - \nabla \log p_{k_2}(\mathbf{x}^{k_2}|\mathbf{y})\|_2^2 \cdot p_{k_2}(\mathbf{x}^{k_2}|\mathbf{y}) d\mathbf{x}^{k_2} \\
&= \mathcal{O} \left(\frac{B^2}{\sigma_k^2} \cdot N^{-\frac{2b}{w_x + w_y}} \cdot (\log N)^{b+1} \right),
\end{aligned} \tag{34}$$

where $\delta \leq k_1 \leq K$ and $0 \leq k_2 \leq K$. The ReLU NN class \mathcal{F} is parameterized by hyperparameters that fulfill

$$M_t = \mathcal{O} \left(\sqrt{\log N} / \sigma_t \right), \quad W = \mathcal{O} (N \log^7 N),$$

$$\kappa = \exp(\mathcal{O}(\log^4 N)), \quad L = \mathcal{O}(\log^4 N), \quad P = \mathcal{O}(N \log^9 N).$$

Proof. See Appendix I. \square

$$\begin{aligned}
d(\mathbf{s}_{c,i}, \mathbf{s}_{c,j}) - d'(\mathbf{s}_{c,i}, \mathbf{s}_{c,j}) &\leq \max_{\mathbf{a} \in \mathcal{A}} C_r \left[W_1(d) \left(\hat{P}(r_{i+1} | \mathbf{s}_{c,i}, \mathbf{a}), \hat{P}(r_{j+1} | \mathbf{s}_{c,j}, \mathbf{a}) \right) - W_1(d') \left(\hat{P}(r_{i+1} | \mathbf{s}_{c,i}, \mathbf{a}), \hat{P}(r_{j+1} | \mathbf{s}_{c,j}, \mathbf{a}) \right) \right] \\
&\quad + \max_{\mathbf{a} \in \mathcal{A}} C_s \left[W_1(d) \left(\hat{P}(s' | \mathbf{s}_{c,i}, \mathbf{a}), \hat{P}(s' | \mathbf{s}_{c,j}, \mathbf{a}) \right) - W_1(d') \left(\hat{P}(s' | \mathbf{s}_{c,i}, \mathbf{a}), \hat{P}(s' | \mathbf{s}_{c,j}, \mathbf{a}) \right) \right] \\
&\leq \max_{\mathbf{a} \in \mathcal{A}} \left[C_r W_1 \|d - d'\|_\infty \left(\hat{P}(r_{i+1} | \mathbf{s}_{c,i}, \mathbf{a}), \hat{P}(r_{j+1} | \mathbf{s}_{c,j}, \mathbf{a}) \right) + C_s W_1 \|d - d'\|_\infty \left(\hat{P}(s' | \mathbf{s}_{c,i}, \mathbf{a}), \hat{P}(s' | \mathbf{s}_{c,j}, \mathbf{a}) \right) \right] \\
&\leq (C_r + C_s) \|d - d'\|_\infty, \quad \forall (\mathbf{s}_{c,i}, \mathbf{s}_{c,j}) \in \mathcal{S}_c \times \mathcal{S}_c.
\end{aligned} \tag{36}$$

Lemma 8. Under Assumption 1, Lemmas 6 and 7, given ReLU NN $\mathcal{F}(M_t, W, \kappa, L, P)$ as Lemma 7, by setting the early-stopping step $k_0 = n^{-\mathcal{O}(1)}$, the network size parameter $N = n^{\frac{1}{w_x + w_y + 2b}}$, and terminal step $K = \mathcal{O}(\log n)$, the empirical loss has

$$\mathbb{E}_{\{\mathbf{x}_{t+1}, \mathbf{y}_t\}} [\mathcal{R}(\varphi)] = \mathcal{O}(\log \frac{1}{k_0} n^{-\frac{2b}{2w_s + w_a + 2b}} (\log n)^{\max(17, b)}). \tag{35}$$

Proof. See Appendix J. \square

Taking expectations w.r.t. n samples $\{\mathbf{x}_t, \mathbf{s}_t, \mathbf{a}_t\}$ and applying (35), we have

$$\begin{aligned}
&\mathbb{E} \left[W_1(P'(\mathbf{x}_{t+1}^{k_0} | \hat{\mathbf{s}}_t, \mathbf{a}_t), \hat{P}(\mathbf{x}_{t+1}^{k_0} | \hat{\mathbf{s}}_t, \mathbf{a}_t)) \right] \\
&\lesssim \mathcal{T}(\mathbf{s}_c^*, \mathbf{a}^*) \sqrt{\frac{K}{2} \frac{1}{k_0} n^{-\frac{2b}{2w_s + w_a + 2b}} (\log n)^{\max(17, b)}}.
\end{aligned}$$

Taking $k_0 = n^{-\frac{4b}{2w_s + w_a + 2b} - 1}$ and $K = \frac{2\beta}{2w_s + w_a + 2b} \log n$, the expected total variation can be bounded as

$$\begin{aligned}
&\mathbb{E} \left[W_1(P'(\mathbf{x}_{t+1}^{k_0} | \hat{\mathbf{s}}_t, \mathbf{a}_t), \hat{P}(\mathbf{x}_{t+1}^{k_0} | \hat{\mathbf{s}}_t, \mathbf{a}_t)) \right] \\
&= \mathcal{T}(\mathbf{s}_c^*, \mathbf{a}^*) \mathcal{O} \left(n^{-\frac{2b}{2w_s + w_a + 2b}} (\log n)^{\max(19/2, (b+2)/2)} \right).
\end{aligned}$$

Finally, the divergence between the estimated conditional distribution $\hat{P}(\mathbf{x}^{k_0} | \mathbf{y})$ and the true conditional data distribution $P(\mathbf{x} | \mathbf{y})$ can be bounded as

$$\begin{aligned}
&\mathbb{E} \left[W_1(P(\mathbf{x} | \mathbf{y}), \hat{P}(\mathbf{x}^{k_0} | \mathbf{y})) \right] \\
&\leq \mathcal{T}(\mathbf{s}_c^*, \mathbf{a}^*) \mathcal{O} \left(n^{-\frac{2b}{2w_s + w_a + 2b}} (\log n)^{\max(19/2, (b+2)/2)} \right).
\end{aligned}$$

The convergence of $\mathbb{E} \left[\|V^\pi(\mathbf{s}_c) - V^\pi(\hat{\mathbf{F}}(\mathbf{o}))\| \right]$ relies on the convergence of $\frac{\ln c_1}{n^{c_2}} n$, since $c_1 = 6$ and $c_2 = \frac{2p_R}{2p_R + w_s + 1} > 0$ in $\mathcal{O}(n^{-\frac{2p_R}{2p_R + w_s + 1}} (\log n)^6)$ and $c_1 = \max\{\frac{19}{2}, \frac{b+2}{2}\} > 0$ and $c_2 = \frac{b}{2w_s + w_a + 2b} > 0$ in $\frac{2C_r + 2C_s}{1 - C_s - C_r} \mathcal{T}(\mathbf{s}_c^*, \mathbf{a}^*) \mathcal{O} \left(n^{-\frac{b}{2w_s + w_a + 2b}} (\log n)^{\max(19/2, (b+2)/2)} \right)$. With L'Hôpital's rule, $\lim_{n \rightarrow \infty} \frac{\ln c_1}{n^{c_2}} n = \lim_{n \rightarrow \infty} \frac{c_1}{c_2^2 n^{c_2}} = 0, \quad \forall c_1, c_2 > 0$. Both $\mathcal{O}(n^{-\frac{2p_R}{2p_R + w_s + 1}} (\log n)^6)$ and $\frac{2C_r + 2C_s}{1 - C_s - C_r} \mathcal{T}(\mathbf{s}_c^*, \mathbf{a}^*) \mathcal{O} \left(n^{-\frac{b}{2w_s + w_a + 2b}} (\log n)^{\max\{19/2, (b+2)/2\}} \right)$ approach zero, as $n \rightarrow \infty$. The value function of the estimated causal state $V^\pi(\zeta(\mathbf{s}))$ in (17) converges to within $2\hat{\epsilon}$ -neighborhood of the ground-truth causal state $V^\pi(\mathbf{s})$, i.e., the neighborhood region of $V^\pi(\mathbf{s})$ with the radius of $\hat{\epsilon}$.

E. Proof of Lemma 3

The existence proof follows that of Remark 1 in Appendix A, only with P replaced by \hat{P} . Given that \mathcal{S}_c is compact by assumption, it follows that $\text{supp}(\hat{P}) \subseteq \mathcal{S}_c$ is compact as (36). Hence, \mathcal{F} satisfies the $(C_r + C_s)$ -contraction property.

Next, we prove the boundedness of the distance. With Lemma 2 and $\text{supp}(\hat{P}) \subseteq \mathcal{S}_c$, we have, $\forall p \geq 1$,

$$\sup_{\mathbf{s}_{c,i}, \mathbf{s}_{c,j} \in \mathcal{S}_c \times \mathcal{S}_c} W_p(\hat{d})(\hat{P}^\pi(\cdot | \mathbf{s}_{c,i}, \mathbf{a}), \hat{P}^\pi(\cdot | \mathbf{s}_{c,j}, \mathbf{a})) \leq \text{diam}(\mathcal{S}_c; \hat{d}).$$

In turn, $\forall (\mathbf{s}_{c,i}, \mathbf{s}_{c,j}) \in \mathcal{S}_c \times \mathcal{S}_c$,

$$\begin{aligned}
d(\mathbf{s}_{c,i}, \mathbf{s}_{c,j}) &= \max_{\mathbf{a} \in \mathcal{A}} \left(C_r W_p(d) (P(r_{i+1} | \mathbf{s}_{c,i}, \mathbf{a}), P(r_{j+1} | \mathbf{s}_{c,j}, \mathbf{a})) \right. \\
&\quad \left. + C_s W_p(d) (P(s' | \mathbf{s}_{c,i}, \mathbf{a}), P(s' | \mathbf{s}_{c,j}, \mathbf{a})) \right) \\
&\leq C_r (r_{\max} - r_{\min}) + C_s \text{diam}(\mathcal{S}_c; d) \\
&\leq C_r (r_{\max} - r_{\min}) / (1 - C_s),
\end{aligned}$$

which follows from Lemma 2 and gives the upper bound as $p \rightarrow \infty$. Subsequently, $\text{diam}(\mathcal{S}_c; d) \leq C_r (r_{\max} - r_{\min}) / (1 - C_s)$. Likewise, $\forall (\mathbf{s}_{c,i}, \mathbf{s}_{c,j}) \in \mathcal{S}_c \times \mathcal{S}_c$, $\text{diam}(\mathcal{S}_c; \hat{d}) \leq C_r (r_{\max} - r_{\min}) / (1 - C_s)$.

F. Proof of Lemma 4

By the Wasserstein triangle inequality [45], we define the respective differences for rewards and transitions in (37). Since d^p is convex, we obtain

$$\begin{aligned}
&W_p(\|d - \hat{d}\|_\infty + d)(\hat{P}(s' | \mathbf{s}_{c,i}, \mathbf{a}), \hat{P}(s' | \mathbf{s}_{c,j}, \mathbf{a})) \tag{38} \\
&\leq (\inf_{\omega \in \Omega} 2^{p-1} \mathbb{E}_{(\mathbf{s}_{c,i}, \mathbf{s}_{c,j}) \sim \omega} [(\|d - \hat{d}\|_\infty + d(\mathbf{s}_{c,i}, \mathbf{s}_{c,j}))^p])^{1/p} \\
&\leq a_p (\|d - \hat{d}\|_\infty^p + W_p^p(d)(\hat{P}(s' | \mathbf{s}_{c,i}, \mathbf{a}), \hat{P}(s' | \mathbf{s}_{c,j}, \mathbf{a})))^{1/p} \\
&\leq a_p (\|d - \hat{d}\|_\infty + W_p(d)(\hat{P}(s' | \mathbf{s}_{c,i}, \mathbf{a}), \hat{P}(s' | \mathbf{s}_{c,j}, \mathbf{a})))^{1/p} \\
&= a_p (\|d - \hat{d}\|_\infty + W_p(d)(\hat{P}(s' | \mathbf{s}_{c,i}, \mathbf{a}), \hat{P}(s' | \mathbf{s}_{c,j}, \mathbf{a}))).
\end{aligned}$$

Similarly, we obtain

$$\begin{aligned}
&W_p(\|d - \hat{d}\|_\infty + d)(\hat{P}(r_{i+1} | \mathbf{s}_{c,i}, \mathbf{a}), \hat{P}(r_{j+1} | \mathbf{s}_{c,j}, \mathbf{a})) \\
&\leq a_p (\|d - \hat{d}\|_\infty + W_p(d)(\hat{P}(r_{i+1} | \mathbf{s}_{c,i}, \mathbf{a}), \hat{P}(r_{j+1} | \mathbf{s}_{c,j}, \mathbf{a}))).
\end{aligned}$$

Due to Lemma 2, we have:

$$W_p(d)(\hat{P}(s' | \mathbf{s}_{c,i}, \mathbf{a}), \hat{P}(s' | \mathbf{s}_{c,j}, \mathbf{a})) \leq \text{diam}(\mathcal{S}_c; d) \tag{39a}$$

$$W_p(d)(\hat{P}(r_{i+1} | \mathbf{s}_{c,i}, \mathbf{a}), \hat{P}(r_{j+1} | \mathbf{s}_{c,j}, \mathbf{a})) \leq \text{diam}(\mathcal{S}_c; d). \tag{39b}$$

The difference in distance can be bounded in (40), where the second inequality holds due to (37), the penultimate inequality inherits from (38), and the last one comes from (39). Similarly,

$$\begin{aligned}
&|W_p(d)(P(r_{i+1} | \mathbf{s}_{c,i}, \mathbf{a}), P(r_{j+1} | \mathbf{s}_{c,j}, \mathbf{a})) \\
&\quad - W_p(\hat{d})(\hat{P}(r_{i+1} | \mathbf{s}_{c,i}, \mathbf{a}), \hat{P}(r_{j+1} | \mathbf{s}_{c,j}, \mathbf{a}))| \\
&\leq a_p \|d - \hat{d}\|_\infty + (a_p - 1) \text{diam}(\mathcal{S}_c; d) + 2\mathcal{E}_\phi.
\end{aligned} \tag{42}$$

Plugging (40) and (42) into the difference between the approximate and the true bisimulation distances yields

$$\begin{aligned}
&|d(\mathbf{s}_{c,i}, \mathbf{s}_{c,j}) - \hat{d}(\mathbf{s}_{c,i}, \mathbf{s}_{c,j})| \\
&\leq \max_{\mathbf{a} \in \mathcal{A}} \left(C_r |W_p(d)(P(r_{i+1} | \mathbf{s}_{c,i}, \mathbf{a}), P(r_{j+1} | \mathbf{s}_{c,j}, \mathbf{a})) \right.
\end{aligned}$$

$$\left| W_p(d) (P(r_{i+1} | \mathbf{s}_{c,i}, \mathbf{a}), P(r_{j+1} | \mathbf{s}_{c,j}, \mathbf{a})) - W_p(d) (\hat{P}(r_{i+1} | \mathbf{s}_{c,i}, \mathbf{a}), \hat{P}(r_{j+1} | \mathbf{s}_{c,j}, \mathbf{a})) \right| \leq 2\mathcal{E}_\phi; \quad (37a)$$

$$\left| W_p(d) (P(\mathbf{s}' | \mathbf{s}_{c,i}, \mathbf{a}), P(\mathbf{s}' | \mathbf{s}_{c,j}, \mathbf{a})) - W_p(d) (\hat{P}(\mathbf{s}' | \mathbf{s}_{c,i}, \mathbf{a}), \hat{P}(\mathbf{s}' | \mathbf{s}_{c,j}, \mathbf{a})) \right| \leq 2\mathcal{E}_\theta \quad (37b)$$

$$\begin{aligned} & |W_p(d) (P(\mathbf{s}' | \mathbf{s}_{c,i}, \mathbf{a}), P(\mathbf{s}' | \mathbf{s}_{c,j}, \mathbf{a})) - W_p(\hat{d}) (\hat{P}(\mathbf{s}' | \mathbf{s}_{c,i}, \mathbf{a}), \hat{P}(\mathbf{s}' | \mathbf{s}_{c,j}, \mathbf{a}))| \\ & \leq |W_p(\hat{d}) (\hat{P}(\mathbf{s}' | \mathbf{s}_{c,i}, \mathbf{a}), \hat{P}(\mathbf{s}' | \mathbf{s}_{c,j}, \mathbf{a})) - W_p(d) (\hat{P}(\mathbf{s}' | \mathbf{s}_{c,i}, \mathbf{a}), \hat{P}(\mathbf{s}' | \mathbf{s}_{c,j}, \mathbf{a}))| \\ & \quad + |W_p(d) (P(\mathbf{s}' | \mathbf{s}_{c,i}, \mathbf{a}), P(\mathbf{s}' | \mathbf{s}_{c,j}, \mathbf{a})) - W_p(d) (\hat{P}(\mathbf{s}' | \mathbf{s}_{c,i}, \mathbf{a}), \hat{P}(\mathbf{s}' | \mathbf{s}_{c,j}, \mathbf{a}))| \\ & \leq |W_p(\hat{d}) (\hat{P}(\mathbf{s}' | \mathbf{s}_{c,i}, \mathbf{a}), \hat{P}(\mathbf{s}' | \mathbf{s}_{c,j}, \mathbf{a})) - W_p(d) (\hat{P}(\mathbf{s}' | \mathbf{s}_{c,i}, \mathbf{a}), \hat{P}(\mathbf{s}' | \mathbf{s}_{c,j}, \mathbf{a}))| + 2\mathcal{E}_\theta \\ & \leq |W_p(\|\hat{d} - d\|_\infty + d) (\hat{P}(\mathbf{s}' | \mathbf{s}_{c,i}, \mathbf{a}), \hat{P}(\mathbf{s}' | \mathbf{s}_{c,j}, \mathbf{a})) - W_p(d) (\hat{P}(\mathbf{s}' | \mathbf{s}_{c,i}, \mathbf{a}), \hat{P}(\mathbf{s}' | \mathbf{s}_{c,j}, \mathbf{a}))| + 2\mathcal{E}_\theta \\ & \leq |a_p\|d - \hat{d}\|_\infty + a_p W_p(d) (\hat{P}(\mathbf{s}' | \mathbf{s}_{c,i}, \mathbf{a}), \hat{P}(\mathbf{s}' | \mathbf{s}_{c,j}, \mathbf{a})) - W_p(d) (\hat{P}(\mathbf{s}' | \mathbf{s}_{c,i}, \mathbf{a}), \hat{P}(\mathbf{s}' | \mathbf{s}_{c,j}, \mathbf{a}))| + 2\mathcal{E}_\theta \\ & \leq a_p\|d - \hat{d}\|_\infty + (a_p - 1)\text{diam}(\mathcal{S}_c; d) + 2\mathcal{E}_\theta \end{aligned} \quad (41)$$

$$\begin{aligned} |V(\mathbf{s}_c) - V(\hat{F}(\mathbf{o}))| & \leq \left| \max_{\mathbf{a} \in \mathcal{A}} \left[\int_{r \in \mathcal{R}} (r(\mathbf{s}_c, \mathbf{a}) P(r | \mathbf{s}_c, \mathbf{a}) - r(\hat{F}(\mathbf{o}), \mathbf{a}) \tilde{P}(r | \hat{F}(\mathbf{o}), \mathbf{a})) dr \right. \right. \\ & \quad \left. \left. + \gamma \left(\int_{\mathbf{s}' \in \mathcal{S}} P(\mathbf{s}' | \mathbf{s}_c, \mathbf{a}) V(\mathbf{s}') d\mathbf{s}' - \int_{\hat{F}(\mathbf{o}') \in \mathcal{S}_c} \tilde{P}(\hat{F}(\mathbf{o}') | \hat{F}(\mathbf{o}), \mathbf{a}) V(\hat{F}(\mathbf{o}')) d\hat{F}(\mathbf{o}') \right) \right] \right| \\ & \leq \max_{\mathbf{a} \in \mathcal{A}} \left| \int_{r \in \mathcal{R}} (r(\mathbf{s}_c, \mathbf{a}) P(r | \mathbf{s}_c, \mathbf{a}) - r(\hat{F}(\mathbf{o}), \mathbf{a}) \tilde{P}(r | \hat{F}(\mathbf{o}), \mathbf{a})) dr \right| \\ & \quad + \max_{\mathbf{a} \in \mathcal{A}} \gamma \left| \int_{\mathbf{s}' \in \mathcal{S}} P(\mathbf{s}' | \mathbf{s}_c, \mathbf{a}) V(\mathbf{s}') d\mathbf{s}' - \int_{\hat{F}(\mathbf{o}') \in \mathcal{S}_c} \tilde{P}(\hat{F}(\mathbf{o}') | \hat{F}(\mathbf{o}), \mathbf{a}) V(\hat{F}(\mathbf{o}')) d\hat{F}(\mathbf{o}') \right| \end{aligned} \quad (43)$$

$$\begin{aligned} & - W_p(\hat{d}) (\hat{P}(r_{i+1} | \mathbf{s}_{c,i}, \mathbf{a}), \hat{P}(r_{j+1} | \mathbf{s}_{c,j}, \mathbf{a})) \Big| \\ & + \max_{\mathbf{a} \in \mathcal{A}} \left(C_s \left| W_p(d) (P(\mathbf{s}' | \mathbf{s}_{c,i}, \mathbf{a}), P(\mathbf{s}' | \mathbf{s}_{c,j}, \mathbf{a})) \right. \right. \\ & \quad \left. \left. - W_p(\hat{d}) (\hat{P}(\mathbf{s}' | \mathbf{s}_{c,i}, \mathbf{a}), \hat{P}(\mathbf{s}' | \mathbf{s}_{c,j}, \mathbf{a})) \right| \right) \\ & \leq C_r \left| a_p\|d - \hat{d}\|_\infty + (a_p - 1)\text{diam}(\mathcal{S}_c; d) + 2\mathcal{E}_\phi \right| \\ & \quad + C_s \left| a_p\|d - \hat{d}\|_\infty + (a_p - 1)\text{diam}(\mathcal{S}_c; d) + 2\mathcal{E}_\theta \right|. \end{aligned}$$

In other words, we have

$$\|d - \hat{d}\|_\infty \leq 2C_r\mathcal{E}_\phi + 2C_s\mathcal{E}_\theta + (C_r + C_s)a_p\|d - \hat{d}\|_\infty + (C_r + C_s)(a_p - 1)\text{diam}(\mathcal{S}_c; d).$$

Applying the supremum over states, we derive

$$\|d - \hat{d}\|_\infty \leq [(C_r + C_s)(a_p - 1)\text{diam}(\mathcal{S}_c; d) + 2C_r\mathcal{E}_\phi + 2C_s\mathcal{E}_\theta] / [1 - (C_r + C_s)a_p].$$

G. Proof of Lemma 5

Define ξ as the measure over \mathcal{S} . Consider a partition $\hat{F}(\mathbf{o}) \in \mathcal{S}_c$, representing a subset of \mathcal{S}_c formed by clustering points within an ϵ -neighborhood such that $\xi(\hat{F}(\mathbf{o})) > 0$. In analogy with the ξ -average finite MDP formulation in [36, Theorem 3.21], we define the reward and dynamics of the ξ -average finite POMDP as follows:

$$\begin{aligned} \tilde{P}(r | \hat{F}(\mathbf{o}), \mathbf{a}) &= \frac{1}{\xi(\hat{F}(\mathbf{o}))} \int_{\mathbf{z} \in \hat{F}(\mathbf{o})} P(r | \mathbf{z}, \mathbf{a}) d\xi(\mathbf{z}); \\ \tilde{P}(\hat{F}(\mathbf{o}') | \hat{F}(\mathbf{o}), \mathbf{a}) &= \frac{1}{\xi(\hat{F}(\mathbf{o}))} \int_{\mathbf{z} \in \hat{F}(\mathbf{o})} P(\hat{F}(\mathbf{o}') | \mathbf{z}, \mathbf{a}) d\xi(\mathbf{z}). \end{aligned}$$

Then, we obtain (43), where the penultimate inequality holds because $r(\mathbf{s}_c, \mathbf{a})$ is 1-Lipschitz and the W_1 metric has dual form; the last line is due to Lemma 1. Similarly, we obtain

(44). where the second inequality holds since $\|\cdot\|_\infty$ defined the supremum norm over \mathcal{S} , the third inequality holds because $\frac{C_r\gamma}{C_s} V(\mathbf{s}_c)$ is 1-Lipschitz, together with the dual form of the W_1 metric, and the last inequality is due to Lemma 1. Hence,

$$\begin{aligned} |V(\mathbf{s}_c) - V(\hat{F}(\mathbf{o}))| & \leq \max_{\mathbf{a} \in \mathcal{A}} (A_1 + A_2) \\ & \leq \frac{C_r^{-1}}{\xi(\hat{F}(\mathbf{o}))} \int_{\mathbf{z} \in \hat{F}(\mathbf{o})} d(\mathbf{s}_c, \mathbf{z}) d\xi(\mathbf{z}) + \gamma \|V - V\|_\infty \\ & \leq C_r^{-1} 2\epsilon + \gamma \|V - V\|_\infty. \end{aligned} \quad (47)$$

Hence, applying the supremum over states:

$$|V(\mathbf{s}_c) - V(\hat{F}(\mathbf{o}))| \leq 2\epsilon / (C_r(1 - \gamma)), \quad \forall \mathbf{s} \in \mathcal{S}. \quad (48)$$

H. Proof of Lemma 6

For any two ReLU NNs, φ_1 and φ_2 , with $\|\varphi_1 - \varphi_2\|_{L_\infty \mathcal{D}} \leq \epsilon$, the L_∞ error is bounded between $\ell(\cdot, \cdot, \varphi_1)$ and $\ell(\cdot, \cdot, \varphi_2)$. For any $(\mathbf{x}, \mathbf{y}) \in \mathcal{D}$, we have (49), where $\hat{\mathbf{x}}^0 = \frac{1}{\sqrt{\alpha_\delta}} (\mathbf{x}^0 - \sqrt{1 - \alpha_\delta} \epsilon)$ and ϵ follows a normal distribution. For the second inequality, we invoke $|\varphi(\mathbf{x}^k, \tau \mathbf{y}, k)| \leq m_k \sqrt{\log N}$. In the last inequality, we invoke $m_k \leq \frac{1}{\sigma_k^2} \leq O(\frac{1}{k})$ when $k = o(1)$ and $m_k = O(1)$ when $k \gg 1$, and have $\log N \lesssim K - \delta$ and $\delta \geq k_0$. Since \mathcal{F} concatenates two ReLU NNs of the identical architecture, the input variable $\mathbf{z} = (\mathbf{x}, \mathbf{y}, k)$ (or $\mathbf{z} = (\mathbf{x}, k)$ in the unconditional setting) lies within the bounded domain $\|(\mathbf{x}, \mathbf{y}, k)\|_\infty \leq \max(R, K)$. By [46, Lemma 7], the covering number of \mathcal{F} is bounded as

$$\mathcal{N}(\varrho, \mathcal{F}, \|\cdot\|_{L_\infty \mathcal{D}}) \lesssim \left(\frac{2L^2(W \max(R, K) + 2)\kappa^L W^{L+1}}{\varrho} \right)^{2P}.$$

Together with (49), we bound the covering number of $\mathcal{S}(R)$.

$$\begin{aligned}
A_1 &= \left| \int_{r \in \mathcal{R}} \left(r(\mathbf{s}_c, \mathbf{a}) P(r | \mathbf{s}_c, \mathbf{a}) - r(\hat{F}(\mathbf{o}), \mathbf{a}) \tilde{P}(r | \hat{F}(\mathbf{o}), \mathbf{a}) \right) dr \right| \\
&\leq \frac{1}{\xi(\hat{F}(\mathbf{o}))} \int_{\mathbf{z} \in \hat{F}(\mathbf{o})} \left| \int_{r \in \mathcal{R}} \left(r(\mathbf{s}_c, \mathbf{a}) P(r | \mathbf{s}_c, \mathbf{a}) - r(\hat{F}(\mathbf{o}), \mathbf{a}) \tilde{P}(r | \hat{F}(\mathbf{o}), \mathbf{a}) \right) dr \right| d\xi(\mathbf{z}) \\
&\leq \frac{C_r^{-1}}{\xi(\hat{F}(\mathbf{o}))} \int_{\mathbf{z} \in \hat{F}(\mathbf{o})} C_r W_1(d) (P(r | \mathbf{s}_c, \mathbf{a}), P(r | \mathbf{z}, \mathbf{a})) d\xi(\mathbf{z}) \leq \frac{C_r^{-1}}{\xi(\hat{F}(\mathbf{o}))} \int_{\mathbf{z} \in \hat{F}(\mathbf{o})} C_r W_p(d) (P(r | \mathbf{s}_c, \mathbf{a}), P(r | \mathbf{z}, \mathbf{a})) d\xi(\mathbf{z})
\end{aligned} \tag{44}$$

$$\begin{aligned}
A_2 &= \gamma \left| \int_{\mathbf{s}' \in \mathcal{S}} P(\mathbf{s}' | \mathbf{s}_c, \mathbf{a}) V(\mathbf{s}') d\mathbf{s}' - \int_{\hat{F}(\mathbf{o}') \in \mathcal{S}_c} \tilde{P}(\hat{F}(\mathbf{o}') | \hat{F}(\mathbf{o}), \mathbf{a}) V(\hat{F}(\mathbf{o}')) d\hat{F}(\mathbf{o}') \right| \\
&\leq \frac{\gamma}{\xi(\hat{F}(\mathbf{o}))} \int_{\mathbf{z} \in \hat{F}(\mathbf{o})} \left| \int_{\mathbf{s}' \in \mathcal{S}} (P(\mathbf{s}' | \mathbf{s}_c, \mathbf{a}) V(\mathbf{s}') - P(\mathbf{s}' | \mathbf{z}, \mathbf{a}) V(\mathbf{s}')) d\mathbf{s}' \right| d\xi(\mathbf{z}) \\
&\quad + \frac{\gamma}{\xi(\hat{F}(\mathbf{o}))} \int_{\mathbf{z} \in \hat{F}(\mathbf{o})} \left| \int_{\mathbf{s}' \in \mathcal{S}} \left(P(\hat{F}(\mathbf{o}') | \mathbf{z}, \mathbf{a}) (V(\mathbf{s}') - V(\hat{F}(\mathbf{o}')) \right) d\mathbf{s}' \right| d\xi(\mathbf{z}) \\
&\leq \frac{\gamma}{\xi(\hat{F}(\mathbf{o}))} \int_{\mathbf{z} \in \hat{F}(\mathbf{o})} \left| \int_{\mathbf{s}' \in \mathcal{S}} (P(\mathbf{s}' | \mathbf{s}_c, \mathbf{a}) - P(\mathbf{s}' | \mathbf{z}, \mathbf{a})) V(\mathbf{s}') d\mathbf{s}' \right| d\xi(\mathbf{z}) + \|V - V\|_\infty \\
&\leq \frac{C_r^{-1}}{\xi(\hat{F}(\mathbf{o}))} \int_{\mathbf{z} \in \hat{F}(\mathbf{o})} C_s \left| \int_{\mathbf{s}' \in \mathcal{S}} (P(\mathbf{s}' | \mathbf{s}_c, \mathbf{a}) - P(\mathbf{s}' | \mathbf{z}, \mathbf{a})) \frac{C_r \gamma}{C_s} V(\mathbf{s}') d\mathbf{s}' \right| d\xi(\mathbf{z}) + \gamma \|V - V\|_\infty \\
&\leq \frac{C_r^{-1}}{\xi(\hat{F}(\mathbf{o}))} \int_{\mathbf{z} \in \hat{F}(\mathbf{o})} C_s W_1(d) (P(\mathbf{s}' | \mathbf{s}_c, \mathbf{a}), P(\mathbf{s}' | \mathbf{z}, \mathbf{a})) d\xi(\mathbf{z}) + \gamma \|V - V\|_\infty \\
&\leq \frac{C_r^{-1}}{\xi(\hat{F}(\mathbf{o}))} \int_{\mathbf{z} \in \hat{F}(\mathbf{o})} C_s W_p(d) (P(\mathbf{s}' | \mathbf{s}_c, \mathbf{a}), P(\mathbf{s}' | \mathbf{z}, \mathbf{a})) d\xi(\mathbf{z}) + \gamma \|V - V\|_\infty,
\end{aligned} \tag{45}$$

$$\begin{aligned}
|\ell(\mathbf{x}, \mathbf{y}, \varphi_1) - \ell(\mathbf{x}, \mathbf{y}, \varphi_2)| &\leq \int_{k_0}^K \frac{1}{K - k_0} \frac{\mathbb{E}}{\tau, \mathbf{x}^k | \mathbf{x}^0 = \hat{\mathbf{x}}^0} \left[\left(\varphi_1(\mathbf{x}^k, \tau \mathbf{y}, k) - \varphi_2(\mathbf{x}^k, \tau \mathbf{y}, k) \right)^\top \left(\varphi_1(\mathbf{x}^k, \tau \mathbf{y}, k) + \varphi_2(\mathbf{x}^k, \tau \mathbf{y}, k) - 2P(\mathbf{x}^k | \hat{\mathbf{x}}^0) \right) \right] dk \\
&\quad + \int_{\delta}^K \frac{1}{K - \delta} \frac{\mathbb{E}}{\tau, \mathbf{x}^k | \mathbf{x}^\delta = \mathbf{x}} \left[\left(\varphi_1(\mathbf{x}^k, \tau \mathbf{y}, k) - \varphi_2(\mathbf{x}^k, \tau \mathbf{y}, k) \right)^\top \left(\varphi_1(\mathbf{x}^k, \tau \mathbf{y}, k) + \varphi_2(\mathbf{x}^k, \tau \mathbf{y}, k) - 2P(\mathbf{x}^k | \mathbf{x}^\delta) \right) \right] dk \\
&\lesssim \epsilon \int_{k_0}^K \frac{1}{K - k_0} \frac{\mathbb{E}}{\tau, \mathbf{x}^k | \mathbf{x}^0 = \hat{\mathbf{x}}^0} \left[\left\| \varphi_1(\mathbf{x}^k, \tau \mathbf{y}, k) + \varphi_2(\mathbf{x}^k, \tau \mathbf{y}, k) - 2P(\mathbf{x}^k | \hat{\mathbf{x}}^0) \right\| \right] dk \\
&\quad + \epsilon \int_{\delta}^K \frac{1}{K - \delta} \frac{\mathbb{E}}{\tau, \mathbf{x}^k | \mathbf{x}^\delta = \mathbf{x}} \left[\left\| \varphi_1(\mathbf{x}^k, \tau \mathbf{y}, k) + \varphi_2(\mathbf{x}^k, \tau \mathbf{y}, k) - 2P(\mathbf{x}^k | \mathbf{x}^\delta) \right\| \right] dk \\
&\lesssim \epsilon \int_{k_0}^K \frac{1}{K - k_0} \frac{\mathbb{E}}{\tau, \mathbf{x}^k | \mathbf{x}^0 = \hat{\mathbf{x}}^0} \left[\left\| m_k \sqrt{\log N} + P(\mathbf{x}^k | \hat{\mathbf{x}}^0) \right\| \right] dk + \epsilon \int_{\delta}^K \frac{1}{K - \delta} \frac{\mathbb{E}}{\tau, \mathbf{x}^k | \mathbf{x}^\delta = \mathbf{x}} \left[\left\| m_k \sqrt{\log N} + P(\mathbf{x}^k | \mathbf{x}^\delta) \right\| \right] dk \\
&\lesssim \frac{\epsilon}{K - k_0} \left(\sqrt{\log N} \int_{k_0}^K m_k dk + \int_{k_0}^K \frac{1}{\sigma_k} dk \right) + \frac{\epsilon}{K - \delta} \left(\sqrt{\log N} \int_{\delta}^K m_k dk + \int_{\delta}^K \frac{1}{\sigma_k} dk \right) \lesssim \epsilon \log N
\end{aligned} \tag{49}$$

I. Proof of Lemma 7

The proposed loss function can be divided as follows:

$$l_1 = \int_{\mathbf{x}^k} \|\varphi(\mathbf{x}^k, \mathbf{y}, k) - \nabla \log P_k(\mathbf{x}^k | \mathbf{y})\|_2^2 P_k(\mathbf{x}^k | \mathbf{y}) d\mathbf{x}^k, \tag{50a}$$

$$\mathbf{x}^\delta \sim P_{\text{data}}(\mathbf{x}^\delta | \mathbf{y}), \quad \forall \delta \leq k \leq K,$$

$$l_2 = \int_{\mathbf{x}^k} \|\varphi(\mathbf{x}^k, \mathbf{y}, k) - \nabla \log P_k(\mathbf{x}^k | \mathbf{y})\|_2^2 P_k(\mathbf{x}^k | \mathbf{y}) d\mathbf{x}^k, \tag{50b}$$

$$\mathbf{x}^0 = (\mathbf{x}^\delta - \sqrt{1 - \bar{\alpha}_\delta} \epsilon) / \sqrt{\bar{\alpha}_\delta} \quad \forall 0 \leq k \leq K.$$

Next, we analyze l_1 and l_2 separately.

Proof of l_1 : For l_1 , each conditional distribution in the forward process satisfies [27, Assumption 3.1]. We obtain (51). With $f \in \mathcal{H}^b(\mathbb{R}^{w_x} \times \mathbb{R}^{w_y}, B)$ and $f(\mathbf{x}_{\text{tr}}, \mathbf{y}) \geq C$ in Assumption 1, there are two constants B' and C' , such that $f^k \in \mathcal{H}^b(\mathbb{R}^{w_x} \times \mathbb{R}^{w_y}, B')$ and $f(\mathbf{x}^k, \mathbf{y}) \geq C'$ hold. Let $C_2 = C_1/(\alpha_k + C_1\sigma_k^2)$, and the conditional density function

$P(\mathbf{x}^k | \mathbf{y}) = \exp(-C_2 \|\mathbf{x}^k\|_2^2 / 2) \cdot f(\mathbf{x}^k, \mathbf{y})$, there is

$$P(\mathbf{x}^k | \mathbf{y}) = \int_{\mathbb{R}^d} \frac{P(\mathbf{x}_{\text{tr}} | \mathbf{y})}{\sigma_k^d (2\pi)^{d/2}} \exp\left(-\frac{\|\sqrt{\alpha_k} \mathbf{x}_{\text{tr}} - \mathbf{x}^k\|_2^2}{2\sigma_k^2}\right) d\mathbf{x}_{\text{tr}}.$$

Therefore, [27, Assumption 3.1] holds $\forall k \geq 0$. Based on [27, Thm 3.4], by replacing K_0 with δ in (50a), we derive

$$l_1 = \mathcal{O}\left(B^2 \cdot N^{-\frac{2b}{w_x + w_y}} \cdot (\log N)^{b+1} / \sigma_k^2\right). \tag{52}$$

Proof of l_2 : Based on DM, we have $\mathbf{x}^0 = \frac{1}{\sqrt{\bar{\alpha}_\delta}} (\mathbf{x}^\delta - \sqrt{1 - \bar{\alpha}_\delta} \epsilon)$ with ϵ following a normal distribution:

$$\epsilon = (\mathbf{x}^\delta - \sqrt{\bar{\alpha}_\delta} \mathbf{x}^0) / \sqrt{1 - \bar{\alpha}_\delta}. \tag{53}$$

With $P(\epsilon) = \exp(-\|\epsilon\|_2^2 / 2) / (2\pi)^{d/2}$, we have

$$P(\epsilon | \mathbf{x}^0, \mathbf{x}^\delta, \mathbf{y}) = \frac{1}{(2\pi)^{d/2}} \exp\left(-\frac{\|\mathbf{x}^\delta - \sqrt{\bar{\alpha}_\delta} \mathbf{x}^0\|_2^2}{2(1 - \bar{\alpha}_\delta)}\right). \tag{54}$$

$$p_t(\mathbf{x}^k|\mathbf{y}) = \int_{\mathbb{R}^d} P(\mathbf{x}_{\text{tr}}|\mathbf{y}) \frac{1}{\sigma_k^d (2\pi)^{d/2}} \exp\left(-\frac{\|\sqrt{\alpha_k} \mathbf{x}_{\text{tr}} - \mathbf{x}^k\|_2^2}{2\sigma_k^2}\right) d\mathbf{x}_{\text{tr}} \quad (51)$$

$$= \exp\left(-\frac{C_1 \|\mathbf{x}^k\|_2^2}{2(\alpha_k + C_1 \sigma_k^2)}\right) \int_{\mathbb{R}^d} \frac{f(\mathbf{x}_{\text{tr}}, \mathbf{y})}{(2\pi)^{d/2} \sigma_k^d} \exp\left(-\frac{\|\mathbf{x}_{\text{tr}} - \sqrt{\alpha_k} \mathbf{x}^k / (\alpha_k + C_1 \sigma_k^2)\|_2^2}{2\sigma_k^2 / (\alpha_k + C_1 \sigma_k^2)}\right) d\mathbf{x}_{\text{tr}} = \exp\left(-\frac{C_1 \|\mathbf{x}^k\|_2^2}{2(\alpha_k + C_1 \sigma_k^2)}\right) f^k(\mathbf{x}^k, \mathbf{y}).$$

With variable substitution, we have

$$P(\mathbf{x}^0|\mathbf{x}^\delta, \mathbf{y}) = \frac{1}{\sigma_\delta^d (2\pi)^{d/2}} \exp\left(-\frac{\|\mathbf{x}^0 - \mathbf{x}^\delta / \sqrt{\alpha_\delta}\|_2^2}{2\sigma_\delta^2}\right). \quad (55)$$

Therefore, $P(\mathbf{x}^0|\mathbf{x}^\delta, \mathbf{y})$ follows a distribution with mean $\mathbf{x}^\delta / \sqrt{\alpha_\delta}$ and covariance $\sigma_\delta \mathbf{I}$, where $\sigma_\delta = \sqrt{(1 - \bar{\alpha}_\delta) / (\bar{\alpha}_\delta)}$. Then, it readily follows that

$$P(\mathbf{x}^0|\mathbf{y}) = \int_{\mathbb{R}^d} P(\mathbf{x}^0|\mathbf{x}^\delta, \mathbf{y}) P(\mathbf{x}^\delta|\mathbf{y}) d\mathbf{x}^\delta \quad (56)$$

$$= \int_{\mathbb{R}^d} P(\mathbf{x}^\delta|\mathbf{y}) \frac{1}{\sigma_\delta^d (2\pi)^{d/2}} \exp\left(-\frac{\|\mathbf{x}^0 - \mathbf{x}^\delta / \sqrt{\alpha_\delta}\|_2^2}{2\sigma_\delta^2}\right) d\mathbf{x}^\delta.$$

As a result, $P(\mathbf{x}^0|\mathbf{y})$ satisfies [27, Assumption 3.1] and leads to [27, Theorem 3.4]. Consequently, we can replace K_0 with 0 and obtain the final conclusion, that is:

$$l_2 = \mathcal{O}\left(B^2 \cdot N^{-\frac{2b}{w_x + w_y}} \cdot (\log N)^{b+1} / \sigma_k^2\right). \quad (57)$$

By summing l_1 in (52) and l_2 in (57), we obtain the final NN approximation error. Lemma 7 is proved.

J. Proof of Lemma 8

Define $\mathcal{N}_R := \mathcal{N}(\varrho, \mathcal{S}(R), \|\cdot\|_{L^\infty \mathcal{D}})$ for brevity. Under the network configuration in Lemma 7, we obtain the following upper bound on the logarithmic covering number:

$$\log \mathcal{N}_R \lesssim N \log^9 N \left(\text{Poly}(\log \log N) + \log^8 N + \frac{1}{\varrho} \right) + \text{Poly}(\log \log N) \log N \log R$$

$$\lesssim N \log^9 N \left(\log^8 N + \log^2 N \log R + \frac{1}{\varrho} \right). \quad (58)$$

Let $\varphi^*(\mathbf{x}, \mathbf{y}, k) = \nabla \log P(\mathbf{x}^k|\mathbf{y})$ be the true score if $\mathbf{y} \neq \emptyset$ and $\varphi^*(\mathbf{x}, \emptyset, k) = \nabla \log P(\mathbf{x}^k)$. Create n i.i.d. ghost samples:

$$(\mathbf{x}'_1, \mathbf{y}'_1), \dots, (\mathbf{x}'_n, \mathbf{y}'_n) \sim P_{\text{data}}(\mathbf{x}^\delta, \mathbf{y}).$$

As $\mathcal{R}_*(\varphi^*) = 0$ and $\mathcal{R}_*(\varphi)$ deviates from $\ell(\varphi)$ merely by a constant independent of φ , it can be readily bounded that

$$\mathcal{R}_*(\varphi) = \mathcal{R}_*(\varphi) - \mathcal{R}_*(\varphi^*) = \ell(\varphi) - \ell(\varphi^*) \quad (59)$$

$$= \frac{1}{n} \mathbb{E}_{\mathbf{x}'_t, \mathbf{y}'_t} \left[\sum_t (\ell(\mathbf{x}'_t, \mathbf{y}'_t; \varphi) - \ell(\mathbf{x}'_t, \mathbf{y}'_t; \varphi^*)) \right].$$

Define $\ell_1 = \frac{1}{n} \sum_t (\ell(\mathbf{x}_{t+1}, \mathbf{y}_t; \varphi) - \ell(\mathbf{x}_{t+1}, \mathbf{y}_t; \varphi^*))$, $\ell_1^{\text{tr}} = \frac{1}{n} \sum_t (\ell^{\text{tr}}(\mathbf{x}_{t+1}, \mathbf{y}_t; \varphi) - \ell^{\text{tr}}(\mathbf{x}_{t+1}, \mathbf{y}_t; \varphi^*))$ and $\ell_2 = \frac{1}{n} \sum_t (\ell(\mathbf{x}'_t, \mathbf{y}'_t; \varphi) - \ell(\mathbf{x}'_t, \mathbf{y}'_t; \varphi^*))$, $\ell_2^{\text{tr}} = \frac{1}{n} \sum_t (\ell^{\text{tr}}(\mathbf{x}'_t, \mathbf{y}'_t; \varphi) - \ell^{\text{tr}}(\mathbf{x}'_t, \mathbf{y}'_t; \varphi^*))$. We decompose $\mathbb{E}_{\mathbf{x}_{t+1}, \mathbf{y}_t} [\mathcal{R}_*(\varphi)]$ into

$$\mathbb{E}_{\mathbf{x}_{t+1}, \mathbf{y}_t} [\mathcal{R}_*(\varphi)] = \mathbb{E}_{\mathbf{x}_{t+1}, \mathbf{y}_t} [\ell_1^{\text{tr}} - \ell_1] + \mathbb{E}_{\mathbf{x}_{t+1}, \mathbf{y}_t} [\mathbb{E}_{\mathbf{x}'_t, \mathbf{y}'_t} [\ell_2 - \ell_2^{\text{tr}}]]$$

$$+ \mathbb{E}_{\mathbf{x}_{t+1}, \mathbf{y}_t} [\mathbb{E}_{\mathbf{x}'_t, \mathbf{y}'_t} [\ell_2^{\text{tr}}] - \ell_1^{\text{tr}}] + \mathbb{E}_{\mathbf{x}_{t+1}, \mathbf{y}_t} [\ell_1], \quad (60)$$

with the four terms on the RHS denoted by B_1, B_2, C , and D .

Bounding B_1 and B_2 : By the definition of $\ell(\mathbf{x}, \mathbf{y}; \varphi)$, (61) holds $\forall \mathbf{x}, \mathbf{y}$ and $\mathbf{s} \in \mathcal{F}$, where we invoke $|\varphi| \lesssim m_k \sqrt{\log N}$ for the first inequality and $1/\sigma_k \lesssim m_k$ for the last line. For $\forall \varphi \in \mathcal{F}$ with φ possibly dependent on (\mathbf{x}, \mathbf{y}) , we obtain (62), where the middle line follows from the sub-Gaussian property of $P(\mathbf{x}|\mathbf{y})$ with Assumption 1, and the third inequality invokes $\mathbb{E}_{\mathbf{x}^k|\mathbf{x}^0=\mathbf{x}} [\|\nabla \log P(\mathbf{x}^k|\mathbf{x}^0)\|_2^2] = 1/\sigma_k^2$ and $\mathbb{E}_{\mathbf{x}^k|\mathbf{x}^\delta=\mathbf{x}} [\|\nabla \log P(\mathbf{x}^k|\mathbf{x}^\delta)\|_2^2] = 1/\sigma_k^2$. Thus, both B_1 and B_2 are bounded by $\mathcal{O}(\exp(-C_1 R^2) RM)$.

Bounding C : For conciseness, we take $\mathbf{z} = (\mathbf{x}, \mathbf{y})$, and write $\ell^{\text{tr}}(\mathbf{x}, \mathbf{y}; \varphi)$ as $\hat{\ell}(\mathbf{z})$ and $\ell^{\text{tr}}(\mathbf{x}, \mathbf{y}; \varphi^*)$ as $\ell^*(\mathbf{z})$. For $\varrho > 0$ to be specified subsequently, consider $\mathcal{J} = \{\ell_1, \dots, \ell_{N_R}\}$ as a minimal ϱ -covering of $\mathcal{S}(R)$ in the L^∞ metric over \mathcal{D} . Let J denote a random index such that $|\hat{\ell} - \ell_J|_\infty \leq \varrho$. Set $u_j = \max \left\{ A, \sqrt{\mathbb{E}_{\mathbf{z}} [\ell_j(\mathbf{z}) - \ell^*(\mathbf{z})]} \right\}$ with $\mathbf{z} \sim P_{\mathbf{x}, \mathbf{y}}$ independent of $(\mathbf{z}_t, \mathbf{z}'_t)_{t \in \mathcal{B}}$. Moreover, we define

$$E = \max_{1 \leq j \leq N_R} \left| \sum_t [(\ell_j(\mathbf{z}_t) - \ell^*(\mathbf{z}_t)) - (\ell_j(\mathbf{z}'_t) - \ell^*(\mathbf{z}'_t))] / u_j \right|.$$

We can bound C as

$$|C| = \left| \mathbb{E}_{\mathbf{z}_t} \left[\frac{1}{n} \sum_t (\hat{\ell}(\mathbf{z}_t) - \ell^*(\mathbf{z}_t)) \right] - \mathbb{E}_{\mathbf{z}'_t} \left[\frac{1}{n} \sum_t (\hat{\ell}(\mathbf{z}'_t) - \ell^*(\mathbf{z}'_t)) \right] \right|$$

$$\leq \left| \frac{1}{n} \mathbb{E}_{\mathbf{z}_t, \mathbf{z}'_t} \left[\sum_{t \in \mathcal{B}} ((\ell_J(\mathbf{z}_t) - \ell^*(\mathbf{z}_t)) - (\ell_J(\mathbf{z}'_t) - \ell^*(\mathbf{z}'_t))) \right] \right| + 2\varrho$$

$$\leq \frac{1}{n} \mathbb{E}_{\mathbf{z}_t, \mathbf{z}'_t} [u_J E] + 2\varrho \leq \frac{1}{2} \mathbb{E}_{\mathbf{z}_t, \mathbf{z}'_t} [u_J^2] + \frac{1}{2n^2} \mathbb{E}_{\mathbf{z}_t, \mathbf{z}'_t} [E^2] + 2\varrho. \quad (63)$$

Let $h_j(\mathbf{z}) = \ell_j(\mathbf{z}) - \ell^*(\mathbf{z})$ and $\hat{h}(\mathbf{z}) = \hat{\ell}(\mathbf{z}) - \ell^*(\mathbf{z})$; define the truncated population loss as $\mathcal{R}_*^{\text{tr}}(\varphi) = \mathbb{E}_{\mathbf{z}} [\hat{h}]$ and the truncated empirical loss as $\hat{\mathcal{R}}_*^{\text{tr}}(\varphi) = \frac{1}{n} \sum_t \hat{h}(\mathbf{z}_t)$. From (62), it follows that $|\mathcal{R}_*^{\text{tr}}(\varphi) - \mathcal{R}_*(\varphi)| \lesssim \exp(-C_1 R^2) RM$.

From the definition of u_j , it follows that

$$\mathbb{E}_{\mathbf{z}_t, \mathbf{z}'_t} [u_J^2] \leq A^2 + \mathbb{E}_{\mathbf{z}_t, \mathbf{z}'_t} [\mathbb{E}_{\mathbf{z}} [h_J(\mathbf{z})]]$$

$$\leq A^2 + \mathbb{E}_{\mathbf{z}_t, \mathbf{z}'_t} [\mathbb{E}_{\mathbf{z}} [\hat{h}(\mathbf{z})]] + 2\varrho$$

$$= A^2 + \mathbb{E}_{\mathbf{z}_t, \mathbf{z}'_t} [\mathcal{R}_*^{\text{tr}}(\varphi)] + 2\varrho. \quad (64)$$

Denote $g_j = \sum_t [h_j(\mathbf{z}_t) - h_j(\mathbf{z}'_t)] / u_j$. Notice that $\mathbb{E}_{\mathbf{z}_t, \mathbf{z}'_t} [(h_j(\mathbf{z}_t) - h_j(\mathbf{z}'_t)) / u_j] = 0, \forall t, j$. With the independence of $\{g_j\}_{j=1}^{N_R}$, we have

$$\mathbb{E}_{\mathbf{z}_t, \mathbf{z}'_t} \left[\sum_t [(h_j(\mathbf{z}_t) - h_j(\mathbf{z}'_t)) / u_j]^2 \right]$$

$$\leq \sum_t \mathbb{E}_{\mathbf{z}_t, \mathbf{z}'_t} \left[(h_j(\mathbf{z}_t) / u_j)^2 + (h_j(\mathbf{z}'_t) / u_j)^2 \right]$$

$$\leq M \sum_t \mathbb{E}_{\mathbf{z}_t, \mathbf{z}'_t} [h_j(\mathbf{z}_t) / u_j^2 + h_j(\mathbf{z}'_t) / u_j^2] \leq 2nM.$$

Since $|(h_j(\mathbf{z}_t) - h_j(\mathbf{z}'_t)) / u_j| \leq M/A$ and g_j has zero mean, applying Bernstein's inequality yields that, $\forall j$, there exists

$$P[g_j^2 \geq h] = 2P \left[\sum_t (h_j(\mathbf{z}_t) - h_j(\mathbf{z}'_t)) / u_j \geq \sqrt{h} \right]$$

$$\begin{aligned}
\ell(\mathbf{x}, \mathbf{y}; \varphi) &\leq 2 \int_{k_0}^T \frac{1}{K-k_0} \mathbb{E}_{\tau, \mathbf{x}^k | \mathbf{x}^0 = \hat{\mathbf{x}}^0} \left[\left\| \varphi(\mathbf{x}^k, \tau \mathbf{y}, k) \right\|_2^2 + \left\| \nabla \log p_t(\mathbf{x}^k | \hat{\mathbf{x}}^0) \right\|_2^2 \right] dk + 2 \int_{\delta}^T \frac{1}{K-\delta} \mathbb{E}_{\tau, \mathbf{x}^k | \mathbf{x}^\delta = \mathbf{x}} \left[\left\| \varphi(\mathbf{x}^k, \tau \mathbf{y}, k) \right\|_2^2 + \left\| \nabla \log p_t(\mathbf{x}^k | \mathbf{x}^\delta) \right\|_2^2 \right] dk \\
&\lesssim \int_{k_0}^T \frac{1}{K-k_0} \mathbb{E}_{\tau, \mathbf{x}^k | \mathbf{x}^0 = \hat{\mathbf{x}}^0} \left[m_t^2 \log N + \left\| \nabla \log p_t(\mathbf{x}^k | \hat{\mathbf{x}}^0) \right\|_2^2 \right] dk + \int_{\delta}^T \frac{1}{K-\delta} \mathbb{E}_{\tau, \mathbf{x}^k | \mathbf{x}^\delta = \mathbf{x}} \left[m_t^2 \log N + \left\| \nabla \log p_t(\mathbf{x}^k | \mathbf{x}^\delta) \right\|_2^2 \right] dk \\
&\lesssim \int_{k_0}^K M_k^2 dk + \int_{k_0}^K \frac{1}{K-k_0} \frac{1}{\sigma_k^2} dk + \int_{\delta}^K M_k^2 dk + \int_{\delta}^K \frac{1}{K-\delta} \frac{1}{\sigma_k^2} dk \lesssim \int_{k_0}^K M_k^2 dk + \int_{\delta}^K M_k^2 dk \lesssim \int_{k_0}^K M_k^2 dk = M, \quad (61)
\end{aligned}$$

$$\begin{aligned}
\mathbb{E}_{\mathbf{x}, \mathbf{y}} [\ell(\mathbf{x}, \mathbf{y}; \varphi) - \ell^{\text{tr}}(\mathbf{x}, \mathbf{y}; \varphi)] &\leq 2 \int_{k_0}^K \frac{1}{K-k_0} \int_{\mathbf{y}} \int_{\|\mathbf{x}\| > R} \mathbb{E}_{\tau, \mathbf{x}^k | \mathbf{x}^0 = \hat{\mathbf{x}}^0} \left[\left\| \varphi(\mathbf{x}^k, \tau \mathbf{y}, k) \right\|_2^2 + \left\| \nabla \log \zeta(\mathbf{x}^k | \mathbf{x}^0) \right\|_2^2 \right] P(\mathbf{x} | \mathbf{y}) P(\mathbf{y}) d\mathbf{x} d\mathbf{y} dk \\
&\quad + 2 \int_{\delta}^K \frac{1}{K-\delta} \int_{\mathbf{y}} \int_{\|\mathbf{x}\| > R} \mathbb{E}_{\tau, \mathbf{x}^k | \mathbf{x}^\delta = \mathbf{x}} \left[\left\| \varphi(\mathbf{x}^k, \tau \mathbf{y}, k) \right\|_2^2 + \left\| \nabla \log \zeta(\mathbf{x}^k | \mathbf{x}^\delta) \right\|_2^2 \right] P(\mathbf{x} | \mathbf{y}) P(\mathbf{y}) d\mathbf{x} d\mathbf{y} dk \\
&\lesssim \int_{k_0}^K \frac{1}{\log N} \int_{\|\mathbf{x}\| > R} \mathbb{E}_{\tau, \mathbf{x}^k | \mathbf{x}^0 = \hat{\mathbf{x}}^0} \left[m_k^2 \log N + \left\| \nabla \log \zeta(\mathbf{x}^k | \mathbf{x}^0) \right\|_2^2 \right] \exp(-C_1 \|\mathbf{x}\|_2^2 / 2) d\mathbf{x} dk \\
&\quad + \int_{\delta}^K \frac{1}{\log N} \int_{\|\mathbf{x}\| > R} \mathbb{E}_{\tau, \mathbf{x}^k | \mathbf{x}^\delta = \mathbf{x}} \left[m_k^2 \log N + \left\| \nabla \log \zeta(\mathbf{x}^k | \mathbf{x}^\delta) \right\|_2^2 \right] \exp(-C'_1 \|\mathbf{x}\|_2^2 / 2) d\mathbf{x} dk \quad (62) \\
&\lesssim \exp(-C_1 R^2) R \int_{k_0}^K m_k^2 dk + \exp(-C_1 R^2) \int_{k_0}^K \frac{1}{\sigma_k^2} dk + \exp(-C'_1 R^2) R \int_{\delta}^K m_k^2 dk + \exp(-C'_1 R^2) \int_{\delta}^K \frac{1}{\sigma_k^2} dk \lesssim \exp(-C_1 R^2) RM
\end{aligned}$$

$$\leq 2 \exp(-(h/2)/(M(2n + \sqrt{h}/3A))).$$

Thus, it follows that

$$P[E^2 \geq h] \leq \sum_{j=1}^{\mathcal{N}_R} P[g_j^2 \geq h] \leq 2\mathcal{N}_R \exp\left(-\frac{h/2}{M(2n + \frac{\sqrt{h}}{3A})}\right).$$

Thus, we have: $\forall h_0 > 0$,

$$\begin{aligned}
\mathbb{E}_{\mathbf{z}_t, \mathbf{z}'_t} [E^2] &= \int_0^{h_0} P[E^2 \geq h] dh + \int_{h_0}^{\infty} P[E^2 \geq h] dh \\
&\leq h_0 + \int_{h_0}^{\infty} 2\mathcal{N}_R \exp\left(-\frac{(h/2)}{M\left(2n + \frac{\sqrt{h}}{3A}\right)}\right) dh \\
&\leq h_0 + 2\mathcal{N}_R \int_{h_0}^{\infty} \left[\exp\left(-\frac{h}{8Mn}\right) + \exp\left(-\frac{3A\sqrt{h}}{4M}\right) \right] dh \\
&\leq h_0 + 2\mathcal{N}_R [8Mn \exp(-h_0/(8Mn)) \\
&\quad + [8M\sqrt{h_0}/(3A) + 32M/(9A^2)] \exp(-3A\sqrt{h_0}/(4M))].
\end{aligned}$$

Taking $A = \sqrt{h_0}/6n$ and $h_0 = 8Mn \log \mathcal{N}_R$, we have

$$\mathbb{E}_{\mathbf{z}_t, \mathbf{z}'_t} [E^2] \leq 8Mn \log \mathcal{N}_R + 48Mn + \frac{32}{\log \mathcal{N}_R} \lesssim Mn \log \mathcal{N}_R. \quad (65)$$

By substituting (64) and (65) into (63), it follows that

$$\begin{aligned}
&\left| \mathbb{E}_{\mathbf{z}_t} [\hat{\mathcal{R}}_\star(\varphi) - \mathcal{R}_\star(\varphi)] \right| \\
&\lesssim \frac{1}{2} (A^2 + \mathbb{E}_{\mathbf{z}_t, \mathbf{z}'_t} [\mathcal{R}_\star^{\text{tr}}(\varphi)] + 2\varrho) + \frac{M}{n} \log \mathcal{N}_R + 2\varrho \\
&= \frac{1}{2} \mathbb{E}_{\mathbf{z}_t} [\mathcal{R}_\star^{\text{tr}}(\varphi)] + \frac{M}{n} \log \mathcal{N}_R + \frac{7}{2} \varrho.
\end{aligned}$$

Thus, we have

$$\mathbb{E}_{\mathbf{z}_t} [\mathcal{R}_\star^{\text{tr}}(\varphi)] \lesssim 2\mathbb{E}_{\mathbf{z}_t} [\hat{\mathcal{R}}_\star(\varphi)] + \frac{M}{n} \log \mathcal{N}_R + 7\delta,$$

which means that

$$\begin{aligned}
C &\lesssim \mathbb{E}_{\mathbf{x}_{t+1}, \mathbf{y}_t} [\ell_1^{\text{tr}}] + \frac{M}{n} \log \mathcal{N}_R + 7\delta \\
&\leq \mathbb{E}_{\mathbf{x}_{t+1}, \mathbf{y}_t} [\ell_1] + |A_1| + \frac{M}{n} \log \mathcal{N}_R + 7\delta \\
&\lesssim D + \exp(-C_1 R^2) RM + (M \log \mathcal{N}_R)/n + 7\delta.
\end{aligned}$$

Bounding D : Let $\hat{\mathcal{R}}_\star(\varphi) = \hat{\ell}(\varphi) - \hat{\ell}(\varphi^\star)$, $\forall \varphi$. Next, $\ell_1 = \hat{\mathcal{R}}_\star(\hat{\mathbf{s}})$. As $\hat{\mathbf{s}}$ is the minimizer of $\hat{\ell}$, it follows

$$\hat{\mathcal{R}}_\star(\varphi) = \hat{\ell}(\hat{\mathbf{s}}) - \hat{\ell}(\varphi^\star) \leq \hat{\ell}(\varphi) - \hat{\ell}(\varphi^\star) = \hat{\mathcal{R}}_\star(\varphi).$$

Thus, we have $D = \mathbb{E}_{\mathbf{z}_t} [\hat{\mathcal{R}}_\star(\varphi)] \leq \mathbb{E}_{\mathbf{z}_t} [\hat{\mathcal{R}}_\star(\varphi)] = \mathcal{R}_\star(\varphi)$.

Take the minimum w.r.t. $\varphi \in \mathcal{F}$. $D \leq \min_{\mathbf{s} \in \mathcal{F}} \mathcal{R}_\star(\varphi)$.

Balancing error: Combining the bounds for B_1 , B_2 , C , and D and plugging the log covering number (58), we derive (66a), where (66c) comes from Assumption 1, $R = \sqrt{\frac{(C_\sigma + 2b) \log N}{C_1(w_x + w_y)}}$ and $\varrho = N^{-2b/(w_x + w_y)}$, and the inequality $M \lesssim \frac{1}{\delta} \leq \frac{1}{k_0} = N^{C_\sigma}$. For any $k > 0$, recall that the score function approximator $\zeta(\cdot, \cdot, k)$ obeys

$$\begin{aligned}
&\mathbb{E}_{\tau, \mathbf{x}^k, \mathbf{y}} \left\| \varphi(\mathbf{x}^k, \tau \mathbf{y}, k) - \nabla \log P(\mathbf{x}^k | \tau \mathbf{y}) \right\|_2^2 \\
&= \frac{1}{2} \int_{\mathbb{R}^d} \|\varphi(\mathbf{x}, \emptyset, k) - \nabla \log P(\mathbf{x})\|^2 P(\mathbf{x}) d\mathbf{x} \\
&\quad + \frac{1}{2} \mathbb{E}_{\mathbf{y}} \left[\int_{\mathbb{R}^d} \|\varphi(\mathbf{x}, \mathbf{y}, k) - \nabla \log P(\mathbf{x} | \mathbf{y})\|^2 P(\mathbf{x} | \mathbf{y}) d\mathbf{x} \right].
\end{aligned}$$

Under Assumption 1, $M = \mathcal{O}(1/k_0)$. Setting $N = n^{(w_x + w_y)/(w_x + w_y + b)}$ and considering Lemma 7, it follows that

$$\mathbb{E}_{\mathbf{z}_t} [\mathcal{R}(\varphi)] \leq 2\mathbb{E}_{\mathbf{z}_t} [\mathcal{R}_\star(\varphi)] \lesssim \frac{1}{t_0} n^{-\frac{b}{w_x + w_y + b}} \log^{\max(17, d+b/2+1)} n.$$

Similarly, under Assumption 1, $M = \mathcal{O}(\log k_0)$. Setting $N = n^{(w_x + w_y)/(w_x + w_y + 2b)}$ and considering Lemma 7, the conditional score error is bounded by

$$\mathbb{E}_{\mathbf{z}_t} [\mathcal{R}(\varphi)] \lesssim \frac{1}{t_0} n^{-\frac{2b}{w_x + w_y + 2b}} \log^{\max(17, (b+1)/2)} n.$$

REFERENCES

- [1] J. Schrittwieser *et al.*, “Mastering atari, go, chess and shogi by planning with a learned model,” *Nature*, vol. 588, no. 7839, pp. 604–609, 2020.
- [2] P. Hansen-Estruch *et al.*, “Bisimulation makes analogies in goal-conditioned reinforcement learning,” in *Proc. Int. Conf. Mach. Learn.*, vol. 162. PMLR, 2022, pp. 8407–8426.
- [3] J. Ho, A. Jain, and P. Abbeel, “Denoising diffusion probabilistic models,” in *Proc. Adv. Neural Inf. Process. Syst.*, vol. 33, 2020, pp. 6840–6851.
- [4] M. Igl *et al.*, “Deep variational reinforcement learning for POMDPs,” in *Proc. Int. Conf. Mach. Learn.*, 2018, pp. 2117–2126.

$$\begin{aligned}
\mathbb{E}_{\mathbf{z}_t} [\mathcal{R}_*(\varphi)] &\leq 2 \min_{\mathbf{s} \in \mathcal{F}} \int_{k_0}^K \frac{1}{K - k_0} \mathbb{E}_{\tau, \mathbf{x}^k, \mathbf{y}} \left\| \varphi(\mathbf{x}^k, \tau \mathbf{y}, k) - \nabla \log P(\mathbf{x}^k | \tau \mathbf{y}) \right\|_2^2 dk \\
&\quad + 2 \min_{\mathbf{s} \in \mathcal{F}} \int_{\delta}^K \frac{1}{K - \delta} \mathbb{E}_{\tau, \mathbf{x}^k, \mathbf{y}} \left\| \varphi(\mathbf{x}^k, \tau \mathbf{y}, k) - \nabla \log P(\mathbf{x}^k | \tau \mathbf{y}) \right\|_2^2 dk \\
&\quad + \mathcal{O} \left(\frac{M}{n} N^{w_x + w_y} \log^9 N \left(\log^8 N + \log^2 N \log R + \frac{1}{\varrho} \right) \right) + \mathcal{O}(\exp(-C_1 R^2) RM) + 7\varrho
\end{aligned} \tag{66a}$$

$$\leq 2 \min_{\mathbf{s} \in \mathcal{F}} \int_{k_0}^K \frac{1}{K - k_0} \mathbb{E}_{\tau, \mathbf{y}} \left[\mathbb{E}_{\mathbf{x}^k} \left\| \varphi(\mathbf{x}^k, \tau \mathbf{y}, k) - \nabla \log P(\mathbf{x}^k | \tau \mathbf{y}) \right\|_2^2 \right] dk \tag{66b}$$

$$+ 2 \min_{\mathbf{s} \in \mathcal{F}} \int_{\delta}^K \frac{1}{K - \delta} \mathbb{E}_{\tau, \mathbf{y}} \left[\mathbb{E}_{\mathbf{x}^k} \left\| \varphi(\mathbf{x}^k, \tau \mathbf{y}, k) - \nabla \log P(\mathbf{x}^k | \tau \mathbf{y}) \right\|_2^2 \right] dk + \mathcal{O} \left(\frac{M}{n} N \log^{17} N \right) + \mathcal{O} \left(N^{-\frac{2b}{w_x + w_y}} \right) \tag{66c}$$

- [5] B. Huang *et al.*, “Action-sufficient state representation learning for control with structural constraints,” in *Proc. Int. Conf. Mach. Learn.*, 2022, pp. 9260–9279.
- [6] M. Janner *et al.*, “Planning with diffusion for flexible behavior synthesis,” in *Proc. Int. Conf. Mach. Learn.*, 2022, pp. 9902–9915.
- [7] A. Ajay *et al.*, “Is conditional generative modeling all you need for decision making?” in *Proc. Int. Conf. Learn. Represent.*, 2022.
- [8] Y. Zhihe and Y. Xu, “DMBP: Diffusion model based predictor for robust offline reinforcement learning against state observation perturbations,” in *Proc. Int. Conf. Learn. Represent.*, 2023.
- [9] T. Lesort *et al.*, “State representation learning for control: An overview,” *Neural Networks*, vol. 108, pp. 379–392, 2018.
- [10] A. Zhang *et al.*, “Learning causal state representations of partially observable environments,” *arXiv preprint arXiv:1906.10437*, 2019.
- [11] A. Zhang, R. T. McAllister, R. Calandra, Y. Gal, and S. Levine, “Learning invariant representations for reinforcement learning without reconstruction,” in *Proc. Int. Conf. Learn. Represent.*, 2020.
- [12] D.-S. Zois, M. Levorato, and U. Mitra, “Active classification for POMDPs: A Kalman-like state estimator,” *IEEE Trans. Signal Processing*, vol. 62, no. 23, pp. 6209–6224, Oct. 2014.
- [13] X. Zhao *et al.*, “ODE-based recurrent model-free reinforcement learning for POMDPs,” in *Proc. Adv. Neural Inf. Process. Syst.*, vol. 36, 2024.
- [14] D. Ha and J. Schmidhuber, “Recurrent world models facilitate policy evolution,” in *Proc. Adv. Neural Inf. Process. Syst.*, vol. 31, 2018.
- [15] M. Lanier *et al.*, “Learning interpretable policies in hindsight-observable POMDPs through partially supervised reinforcement learning,” *arXiv preprint arXiv:2402.09290*, 2024.
- [16] F. Chen *et al.*, “Lower bounds for learning in revealing POMDPs,” in *Proc. Int. Conf. Mach. Learn.*, 2023, pp. 5104–5161.
- [17] A. M. Karimi Mamaghan, A. Dittadi *et al.*, “Diffusion-based causal representation learning,” *Entropy*, vol. 26, no. 7, p. 556, 2024.
- [18] A. Komanduri, C. Zhao, F. Chen *et al.*, “Causal diffusion autoencoders: Toward counterfactual generation via diffusion probabilistic models,” in *Proc. Eur. Conf. Artif. Intell.* IOS Press, 2024, pp. 2516–2523.
- [19] I. Bica, D. Jarrett, and M. van der Schaar, “Invariant causal imitation learning for generalizable policies,” in *Proc. Adv. Neural Inf. Process. Syst.*, vol. 34, 2021, pp. 3952–3964.
- [20] K. Lee, Z. Wang, B. Vlahov, H. Brar, and E. A. Theodorou, “Ensemble bayesian decision making with redundant deep perceptual control policies,” in *Proc. Int. Conf. Mach. Learn. Appl.*, 2019, pp. 831–837.
- [21] K. Renz *et al.*, “Plant: Explainable planning transformers via object-level representations,” in *Proc. Conf. Robot Learn.*, 2023, pp. 459–470.
- [22] R. Akrouf, F. Veiga, J. Peters, and G. Neumann, “Regularizing reinforcement learning with state abstraction,” in *Proc. IEEE/RSJ Int. Conf. Intell. Robots Syst.*, 2018, pp. 534–539.
- [23] P. Sermanet, C. Lynch, Y. Chebotar, J. Hsu, E. Jang, S. Schaal, S. Levine, and G. Brain, “Time-contrastive networks: Self-supervised learning from video,” in *Proc. Int. Conf. Robot. Automat.*, 2018, pp. 1134–1141.
- [24] C. Han, D. Basu, M. Mangan, E. Vasilaki, and A. Gilra, “Dynamical-vae-based hindsight to learn the causal dynamics of factored-POMDPs,” *arXiv preprint arXiv:2411.07832*, 2024.
- [25] R. Cannizzaro and L. Kunze, “Car-despot: Causally-informed online pomdp planning for robots in confounded environments,” in *Proc. IEEE/RSJ Int. Conf. Intell. Robots Syst.*, 2023, pp. 2018–2025.
- [26] L. Yang, Z. Huang, F. Lei, Y. Zhong, Y. Yang, C. Fang, S. Wen, B. Zhou, and Z. Lin, “Policy representation via diffusion probability model for reinforcement learning,” *arXiv preprint arXiv:2305.13122*, 2023.
- [27] H. Fu, Z. Yang, M. Wang, and M. Chen, “Unveil conditional diffusion models with classifier-free guidance: A sharp statistical theory,” *arXiv preprint arXiv:2403.11968*, 2024.
- [28] C. Villani, *Optimal Transport: Old and New*. Springer Science & Business Media, 2008, vol. 338.
- [29] I. Olkin *et al.*, “The distance between two random vectors with given dispersion matrices,” *Linear Algebra Appl.*, vol. 48, pp. 257–263, 1982.
- [30] F. Santambrogio, “Optimal transport for applied mathematicians,” *Birkhäuser, NY*, vol. 55, no. 58–63, p. 94, 2015.
- [31] R. Givan, T. Dean, and M. Greig, “Equivalence notions and model minimization in Markov decision processes,” *Artificial Intelligence*, vol. 147, no. 1–2, pp. 163–223, 2003.
- [32] P. S. Castro, P. Panangaden, and D. Precup, “Equivalence relations in fully and partially observable Markov decision processes,” in *Proc. Int. Joint Conf. Artif. Intell.*, 2009, pp. 1653–1658.
- [33] A. Q. Nichol and P. Dhariwal, “Improved denoising diffusion probabilistic models,” in *Proc. Int. Conf. Mach. Learn.*, 2021, pp. 8162–8171.
- [34] P. Vincent, “A connection between score matching and denoising autoencoders,” *Neural Computation*, vol. 23, no. 7, pp. 1661–1674, 2011.
- [35] P. S. Castro, “Scalable methods for computing state similarity in deterministic Markov decision processes,” in *Proc. AAAI Conf. Artif. Intell.*, vol. 34, 2020, pp. 10 069–10 076.
- [36] N. Ferns, P. Panangaden, and D. Precup, “Bisimulation metrics for continuous Markov decision processes,” *SIAM J. Comput.*, vol. 40, no. 6, p. 1662–1714, Dec. 2011.
- [37] M. Kohler and A. Krzyżak, “On the rate of convergence of a deep recurrent neural network estimate in a regression problem with dependent data,” *Bernoulli*, vol. 29, no. 2, pp. 1663–1685, 2023.
- [38] H. Chen, Y. Ren, L. Ying, and G. M. Rotskoff, “Accelerating diffusion models with parallel sampling: Inference at sub-linear time complexity,” in *Proc. Adv. Neural Inf. Process. Syst.*, 2024.
- [39] T. Ni, B. Eysenbach, and R. Salakhutdinov, “Recurrent model-free rl can be a strong baseline for many POMDPs,” in *Proc. Int. Conf. Mach. Learn.*, 2022, pp. 16 691–16 723.
- [40] J. N. Yan *et al.*, “Diffusion models without attention,” in *Proc. IEEE Conf. Comput. Vis. Pattern Recognit.*, 2024, pp. 8239–8249.
- [41] A. T. Bharucha-Reid, “Fixed point theorems in probabilistic analysis,” *Bulletin of the American Mathematical Society*, vol. 82, no. 5, pp. 641–657, 1976.
- [42] C. L. Canonne, “A short note on an inequality between KL and TV,” *arXiv preprint arXiv:2202.07198*, 2022.
- [43] S. Chen, S. Chewi, J. Li, Y. Li, A. Salim, and A. R. Zhang, “Sampling is as easy as learning the score: theory for diffusion models with minimal data assumptions,” in *Proc. Int. Conf. Learn. Represent.*, 2023.
- [44] J. Fan, Z. Wang, Y. Xie, and Z. Yang, “A theoretical analysis of deep Q-learning,” in *Learn. dynamics Control*, 2020, pp. 486–489.
- [45] P. Clement and W. Desch, “An elementary proof of the triangle inequality for the Wasserstein metric,” in *Proc. Amer. Math. Soc.*, vol. 136, no. 1, 2008, pp. 333–339.
- [46] M. Chen *et al.*, “Nonparametric regression on low-dimensional manifolds using deep ReLU networks: Function approximation and statistical recovery,” *IMA Inf. Inf.*, vol. 11, no. 4, pp. 1203–1253, Dec. 2022.